



Digital Commons@

Loyola Marymount University
LMU Loyola Law School

Biology Theses

Biology

Fall 2022

Teratogenic Effects of Cannabinoid and Serotonin Receptor Disruption on Neural Crest Development

Brian K. Wells

Loyola Marymount University, brian.kai.wells@gmail.com

Follow this and additional works at: https://digitalcommons.lmu.edu/bio_thesis



Part of the [Biology Commons](#)

Recommended Citation

Wells, Brian K., "Teratogenic Effects of Cannabinoid and Serotonin Receptor Disruption on Neural Crest Development" (2022). *Biology Theses*. 1.

https://digitalcommons.lmu.edu/bio_thesis/1

This Thesis is brought to you for free and open access by the Biology at Digital Commons @ Loyola Marymount University and Loyola Law School. It has been accepted for inclusion in Biology Theses by an authorized administrator of Digital Commons@Loyola Marymount University and Loyola Law School. For more information, please contact digitalcommons@lmu.edu.



Loyola Marymount University
Frank R. Seaver
College of Science
and Engineering

TERATOGENIC EFFECTS OF CANNABINOID AND SEROTONIN RECEPTOR DISRUPTION ON NEURAL CREST DEVELOPMENT

A thesis submitted in partial satisfaction
of the requirements of the Biology Department
of Loyola Marymount University

by

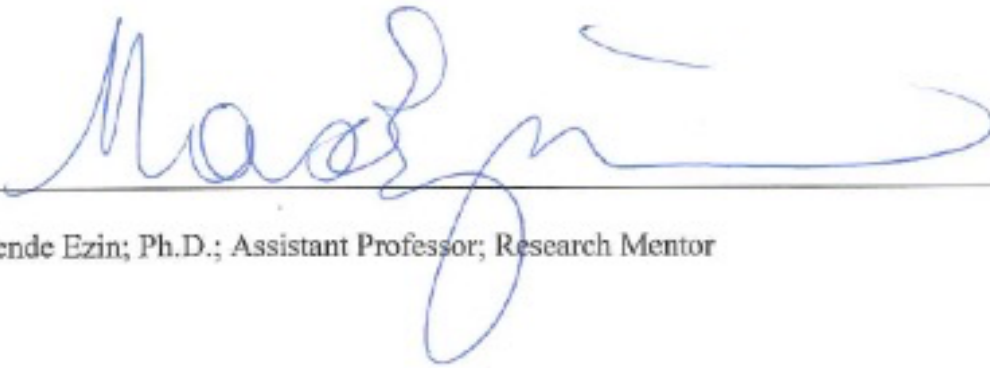
Brian K. Wells

December 20, 2022

Signature Page



Brian Wells; BS candidate; Rains Research Assistant



Maxellende Ezin; Ph.D.; Assistant Professor; Research Mentor

© 2022

Brian K. Wells

ALL RIGHTS RESERVED

For my mom, dad, and sister

Mary, Bill, and Chelsea

Acknowledgments

I wouldn't have been able to accomplish anything in this thesis if it wasn't for the support of everyone in the Ezin lab. Thank you to Amira, Christina, Halley, Chloe, Gwyneth, Perla, Dr. Evans, Dr. de Bellard, and most of all, Dr. Ezin. When I entered Dr. Ezin's lab, I knew I wanted to work in science, but I didn't know where to start. Thanks almost entirely to her guidance, I have taken my first steps in that direction. Additionally, thank you to Gwyneth and Amira for their pivotal contributions to Chapter 2.

Abstract

Neurotransmitters are well-studied in adults and have often been the focus of many treatments for both physical and psychological ailments. This thesis explores the teratogenicity of altering the activity at the serotonin 2B and 2C receptors (5-HT2B; 5-HT2C) and the cannabinoid 1 receptor (CB1R) in the serotonergic and endocannabinoid systems, respectively. This investigation is focused on neural crest derivative structures. Chapter 1 reviews the background information behind cardiac and cranial neural crest cells and overviews the serotonergic and endocannabinoid systems.

In Chapter 2, using a pharmacological agent, 1-methylpsilocin (1-MP), we disrupt the activity of 5-HT2B and 5-HT2C in the early development of chicken embryos. The results indicate that this disruption leads to altered migration patterns in cardiac neural crest cells (cNCC) at Hamburger-Hamilton stage (HH) 14. At HH32 and HH36, embryos exposed to 1-MP show defects in cardiac neural crest derivative structures. These results suggest a novel activity of the 5-HT2B receptor on the migration of cNCC.

In Chapter 3, we investigate the impact of altering the activity of the CB1R in early avian development by applying a CB1R agonist. Our results reveal that overactivation of the CB1R results in defects in cranial neural crest migration and derivative structures. A non-muscle myosin II ATPase inhibitor informs on the mechanism for the CB1R-induced altered migration pattern.

In Chapter 4, we discuss the broader societal impacts of these findings. I propose that these results indicate a need for further investigation into the safety of 5-HT2B and CB1 receptor disruption in embryonic development.

Parts of the results of this dissertation have been
submitted for publication to The Journal of Morphology /

November 2022

Table of Contents

Abstract	6
Chapter 1: Introduction	10
1.1 Neural Crest Cells	11
1.2 Serotonin	18
1.3 Endocannabinoids	20
Chapter 2: Serotonin 2B and 2C receptor disruption leads to cardiac neural crest defects	23
2.1 Introduction	24
2.2 Materials and Methods	24
2.3 Results	28
2.4 Discussion	31
2.5 Figures	35
Chapter 3: Cannabinoid Receptor Type 1 regulates migration and morphogenesis of cranial neural crest	41
3.1 Introduction	42
3.2 Materials and Methods	42
3.3 Results	46
3.4 Discussion	50
3.5 Conclusion	55
3.6 Figures	56
Chapter 4: Discussion	60
References	63

Chapter 1:

Introduction

1.1 Neural Crest Cells

Neural crest cells (NCCs), a multipotent cell population specific to vertebrates, originate from the dorsal-most portion of the neural tube, migrate ventrally via the anterior-posterior axis, and contribute to a variety of tissues, such as the enteric nervous system, the cartilage, and bones of the face, melanocytes, and the peripheral nervous system (Trainor, 2005). A precise mix of bone morphogenetic protein (BMP), Wnt, fibroblast growth factor (FGF), retinoic acid, and Notch signals provided by the ectoderm, the neuroepithelium, and the underlying mesoderm induce the neural crest (NC) in the neural plate border region (**Fig. 1.1**) (Milet and Monsoro-Burq, 2012; Prasad et al., 2012). Collectively, these signals induce a set of transcription factors, including those produced by the Snail/Slug, Foxd3, and SoxE genes, that define the NC region and regulate further NC growth (Cheung et al., 2005; McKeown et al., 2013; Theveneau and Mayor, 2012).

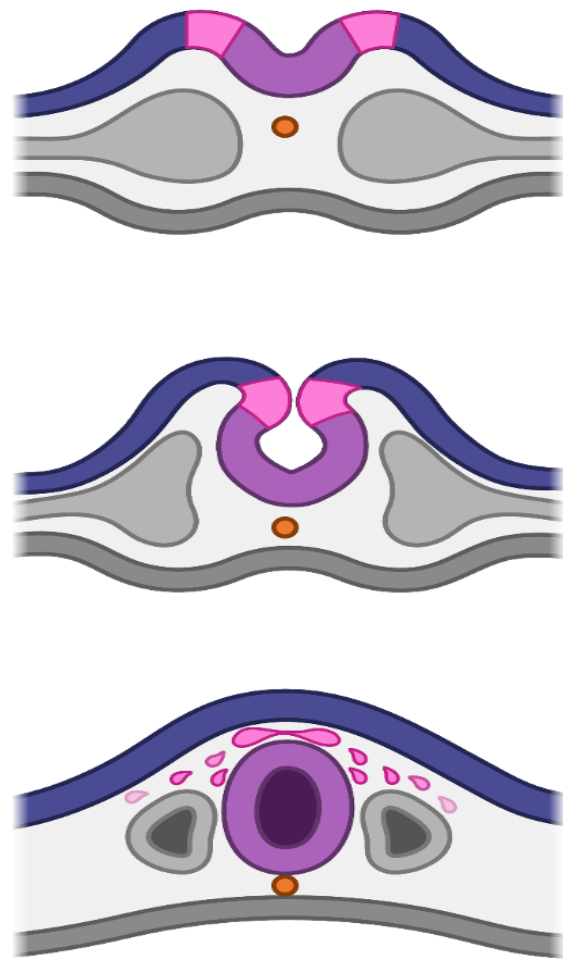


Figure 1.1. Induction and delamination of neural crest cells. The neural plate border (pink) is located between the neuroectoderm (purple), and non-neuroectoderm (blue). The neural tube is formed during neurulation by the elevation of neural folds, the apical constriction of neural plate cells directly above the notochord (orange). Neural crest cells (pink) delaminate and migrate to different areas of the embryo. Created with Biorender.com 2022.

NC migration commences with a full or partial EMT, which permits NC cells to separate from the neuroepithelium and ectoderm (Duband, 2010; Theveneau and Mayor, 2012). At the time of neural induction, a global switch from E-cadherin (cadherin 1) to N-cadherin (cadherin 2) expression occurs (Dady et al., 2012; Nandadasa et al., 2009). As a result, the neural plate and all pre-migratory NC cells express high levels of N-cadherin, with residual levels of E-cadherin primarily found in the cephalic region. This is followed by a switch from high to low N-cadherin expression and the *de novo* expression of weaker cadherins of type II (6/7/11; Cheung et al., 2005). This is regulated in trunk NC cells by Snail/Slug, Foxd3, and Sox9/10 (McKeown et al., 2013); however, in the head, additional factors such as Ets1, LSox5, and p53 are necessary (Perez-Alcala et al., 2004; Rinon et al., 2011; Théveneau et al., 2007). In addition, migratory NC cells secrete proteases capable of cleaving cadherins, such as ADAM10 and ADAM13, further altering their cell-cell adhesion state (McCusker et al., 2009; Shoal et al., 2007). These modifications, along with an alteration in integrin activity and a local reorganization of the extracellular matrix (ECM), induce NC migration.

Regarding the extent of the NC's multipotency, there is still some disagreement despite extensive investigation. Although experimental evidence suggests that the great majority of NC cells are not predefined and differentiate in response to the signals they receive during migration, certain NC cells appear to be committed to a specific lineage prior to the beginning of migration (Krispin et al., 2010; McKinney et al., 2013). Thus, the NC population appears to consist of cells with varying degrees of multipotency and plasticity. Many of the early genes that are upregulated in NC cells in response to induction also regulate the EMT, which initiates migration. Interestingly, EMT has been connected to the acquisition of stem cell properties

(Chang et al., 2011; Mani et al., 2008; Morel et al., 2008). This presents the fascinating idea that NC multipotency and the start of NC migration could be linked and managed simultaneously as part of an EMT program.

The cardiac neural crest

Cardiac neural crest cells (cNCCs) are the subset of NCCs that give rise to cardiac structures, such as the interventricular septum, the cardiac outflow tract, and the heart's semilunar valves (Jain et al. 2011). These cells develop in the neural folds between the otic vesicle and the fourth somite, a region that corresponds to rhombomeres 6 to 8 of the hindbrain in birds and mammals (Kirby 1987). Cardiac NCCs then move toward the caudal pharyngeal arches (PAs; the 3rd, 4th, and 6th PAs). In zebrafish, the cardiac neural crest is found from the otic vesicle to somite 6 (George et al. 2020), and in the heart, cNCCs in zebrafish give rise only to myocardium in the heart; this differs from cNCC derivatives in mammals and birds, detailed below.

Cardiac neural crest cells are indispensable for the normal reorganization of the bilaterally symmetrical pharyngeal arch arteries into the asymmetric great arteries of the thorax. Additionally, the cells support the growth of the thymus and parathyroid glands. The rhombomere 6 subpopulation of cardiac neural crest cells in the caudal pharyngeal arches migrates into the cardiac outflow tract, pausing as it reaches the circumpharyngeal ridge (**Fig. 1.2**; Kuratani and Kirby 1991). At the junction of the presumptive subaortic and sub-pulmonary

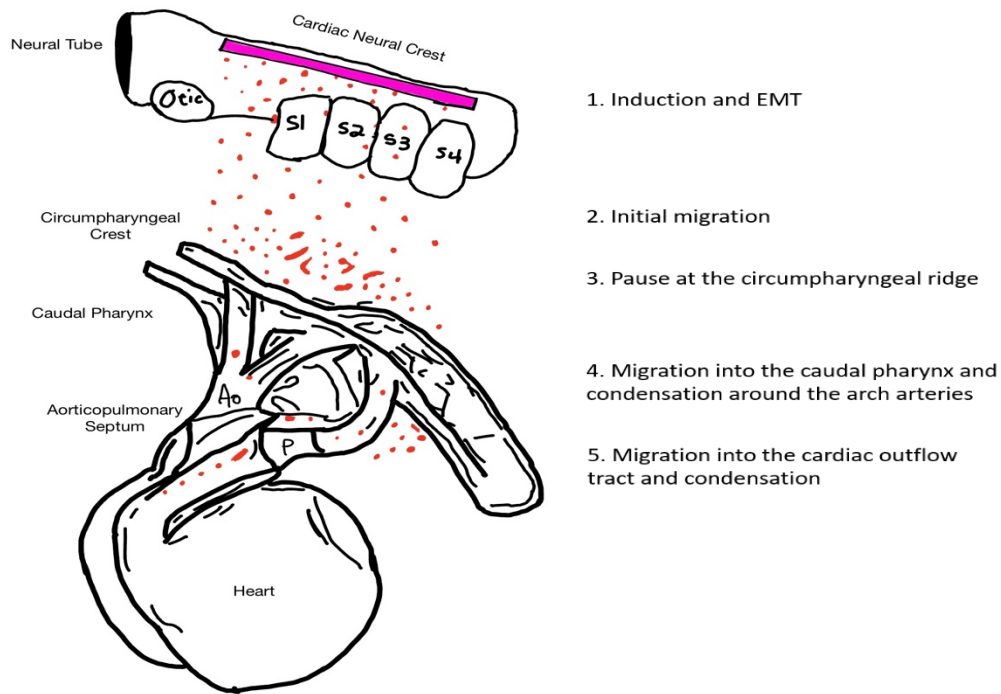


Figure 1.2. Diagram summarizing the stages of cardiac neural crest migration and condensation. Cardiac neural crest cells (red) are induced and undergo an epithelial at the neural tube between the otic vesicle and somite 4 (magenta). They then migrate to the circumpharyngeal ridge, pause, then continue into the caudal pharynx and condense around the pharyngeal arch arteries. After, the cardiac neural crest cells migrate into the cardiac outflow tract and condenses, separating the aorta (Ao) and the pulmonary artery (P). (Adapted from Kirby and Hutson 2010).

Abbreviations. Otic, otic vesicle; S, somite; Ao, aorta; P, pulmonary artery; EMT, epithelial-to-mesenchymal transition.

myocardium of the outflow tract, the cardiac crest forms (1) cardiac ganglia and (2) condensed mesenchyme (Waldo et al. 1998). This condensed mesenchyme is referred to as the aortopulmonary septation complex, which divides: (1) the most distal outflow into the base of the aorta and pulmonary trunks, and (2) the middle outflow into the aortic and pulmonary semilunar valve regions. Cardiac crest cells also migrate into the most proximal outflow tract, where they participate in the final closure of the interventricular septum (Waldo et al. 1998).

The mechanisms by which cNCCs move through the PAs have been explained through several models, including the "contact inhibition of locomotion" model, where two NCCs collide and change direction (Roycroft and Mayor 2016); the "trailblazer cell" model, where gene expression changes in leading cells prompt follower cells to move (McLennon et al. 2015); the "chemoattractant and repellent" model, where signaling molecules from surrounding tissues guide cNCCs (Hutson et al. 2006); and the "co-attraction model," where factors expressed by cNCCs maintain their cohesion via chemotaxis during migration (Carmona-Fontaine et al. 2011). Various gene pathways have been identified to play roles in these processes that drive cNCC migration, such as *FoxD3* (Dottori et al. 2001), *Sox10* (Britsch et al. 2001), *Dvl2* (Hamblet et al. 2002), *Cdh2* (N-cadherin) (Luo et al. 2006), and *Vangl1/Vangl2* (Pryor et al. 2014).

Specific abnormalities and myocardial dysfunction patterns occur in the chick cNCC ablation model, where the number of cardiac neural crest cells migrating to the aortic sac was reduced (by at least half), leading to a number of septal defects. These defects include truncus arteriosus, double outlet of the right ventricle, and interventricular septum defects (Kirby and Creazzo, 1995). The abnormalities consist of a persisting truncus arteriosus and an aberrant repatterning of the bilaterally symmetrical aortic arch arteries to the great arteries (Bockman et al. 1987, 1989). As early as stage 14, the earliest sign of abnormal morphogenesis, the primary alteration in myocardial function, can be seen. This occurs far before cardiac neural crest cells contact the myocardium in an unperturbed embryo (Waldo et al., 1996, 1998). In an embryo in which the section of neural folds that generate cardiac crest cells have been ablated,

the initial myocardial functional anomalies include (1) reduced ejection fraction, (2) decreased calcium current, and (3) aberrant excitation-contraction coupling (Leatherbury et al., 1991; Creazzo, 1990; Creazzo et al., 1997). The same functional defect in the myocardium is observed in mouse embryos with impaired neural crest migration (Conway et al. 1997). During this phase of normal development, neural crest cells interact with endothelial cells of the aortic arch arteries, endodermal, and ectodermal cells of the ventral pharynx (Waldo et al. 1996).

The cranial neural crest

In the developing head, another subtype of neural crest, cranial neural crest cells (CrNCCs), originate in the midbrain and hindbrain (rhombomere (r) segments r1–r8) and migrate along discrete pathways. Disruption of the migration of neural crest cells from the hindbrain region begins in the chick at approximately the five- to six-somite stage (Tosney 1982), in the mouse at the five-somite stage (Nichols 1986), in *Xenopus* around stage 12 (Sadaghiani and Thiebaud, 1987), and in zebrafish at 13–14 hr postfertilization (Schilling and Kimmel 1994). Rhombomeres (r)1 and (r)2 generate numerous neural crest cells, which comigrate ventrolaterally as a collective stream with midbrain-derived neural crest cells and populate the proximodistal extent of the first branchial arch in great numbers (ba1; Lumsden et al. 1991). In the mouse, zebrafish, and *Xenopus*, r3 produces fewer neural crest cells than r1 and r2, and instead of migrating laterally, some r3-derived neural crest cells migrate anteriorly to join the r2 stream (Sechrist et al. 1993; Schilling and Kimmel 1994).

The branchial arch ectoderm is morphologically continuous until it abuts the neural tube. It is reasonable to state that r3-derived neural crest cells in chicken embryos contribute to only the most proximal region of ba1, which corresponds to the trigeminal (semilunar) ganglion of

the V cranial nerve (Kontges and Lumsden 1996). R3-derived neural crest cells contribute to more distal portions of the mandibular arch (ba1) in mouse, zebrafish, and *Xenopus* (Sadaghiani and Thiebaud, 1987; Osumi-Yamashita et al. 1994; Schilling and Kimmel 1994). Thus, in the hindbrain of chick embryos, r1- and r2-derived neural crest cells populate ba1, whereas, in mouse, zebrafish, and *Xenopus*, r3 also contributes a small number of neural crest cells (Trainor and Tam 1995).

Cranial NCCs migrate as dense multicellular streams with distinguishable leader and trailing cells (McLennan et al. 2015). NCC streams are arranged according to chemotaxis and a variety of physical and molecular environmental cues (Shellard et al. 2018). Within the stream, the trajectory of movement polarizes protrusive activity, resulting in the directed migration of individual chick cranial NCCs (Genuth et al. 2018), whereas collectively migrating *Xenopus* NCCs also achieve directed movement via contact-inhibition-locomotion (Carmona-Fontaine et al. 2008; Theveneau et al. 2010). Cranial NCCs communicate with each other via cell contact (Piacentino et al. 2020), and exchange information directly via thin filopodial extensions (McKinny et al. 2011) and gap junctions (Huang et al. 1998) as they migrate. In addition, cranial NCCs undergo macropinocytosis and absorb environmental material, likely for the purpose of guidance (Li et al. 2020). Failure of cranial NCC migration results in significant morphological abnormalities of craniofacial structures and improper innervation of the face (Siismets and Hatch 2020), making this an important model system for understanding congenital craniofacial anomalies.

1.2 Serotonin

Serotonin (also known as 5-hydroxytryptamine or 5-HT) is involved in many different adult physiological processes, such as the regulation of mood, cognition, circadian rhythms, sleep-wake cycles, pain perception, appetite, the manifestation of nausea, and sexual behavior (Jenkins et al. 2016). Serotonin receptors, a type of G-protein coupled receptors (Fig. 1.3), are diverse and the number of different serotonin receptors subtypes varies between animal species. Accumulating *in vitro* evidence also suggests that serotonin signaling regulates development in several animal phyla before neurogenesis (Matthews and Levin 2017).

Serotonin plays a role in the migration of neural crest cells in the mouse model (Moiseiwitsch and Lauder, 1995). In chickens, rats, and mice, serotonin influences craniofacial, gastrointestinal, and cardiovascular morphogenesis; these effects are frequently mediated by the serotonin 2B (5-HT2B) receptor (Buznikov et al. 2001). 5-HT operates as a humoral morphogen based on the concentration of the 5-HT, serotonin receptors, and its transporter (SERT) during development and the capacity

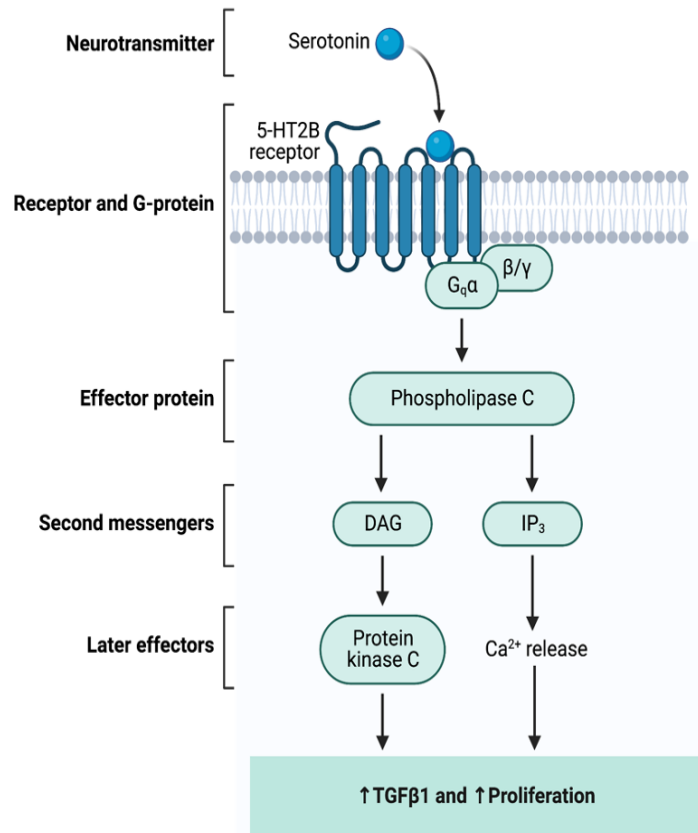


Figure 1.3. 5-HT2B receptor transduction pathway upregulates TGFβ1 and proliferation factors. Figure adapted from “GPCR Effector Pathways” by Biorender.com 2022. Retrieved from <https://app.biorender.com/biorender-templates>

of substances that affect serotonergic transmission to inhibit cranial and cardiac development (Lauder and Zimmerman 1988).

Serotonin plays a role in the development of head mesenchyme and pharyngeal arch, the closure of the neural tube, and the development of the eye and heart, and partially overlaps with retinoic acid teratology (Lauder and Zimmerman 1988). The administration of ritanserin, a highly specific 5-HT_{2B} and 5-HT_{2C} antagonist, to murine embryos, altered the differentiation program of cardiac stem cells and inhibited the migration of the progenitors of trabecular cells (Choi et al. 1997). However, the influence of receptors 5-HT_{2B} and 5-HT_{2C} on cNCCs and their derivative structures was not investigated (Choi et al. 1997).

1.3 Endocannabinoids

The endocannabinoid system (known as the phytocannabinoid system in plants) plays a wide range of functions in plants, fungi, and animals (McPartland et al., 2006; Silver, 2019; Gülck & Møller, 2020). In plants, phytocannabinoid signaling is active in UV protection (Arif et al., 2021). In vertebrates,

endocannabinoid signaling has functions both in the embryonic period and in adulthood, including gametogenesis (Taylor et al., 2007; Oltrabella et al., 2017; Fonseca et al., 2009), neuronal circuit formation (Watson et al., 2008; Berghuis et al., 2007), immune response (Almogi-Hazan & Or, 2020), mood, learning and memory (Kruk-Slomka et al., 2017). The endocannabinoid signaling system involves the lipid cannabinoid (CB) CB1 and CB2 receptors, G-protein coupled transmembrane receptors that can

homodimerize or heterodimerize with each other (Fig. 1.4) (Callen et al., 2012) and with other proteins (Mackie, 2005). The CB receptors are activated extracellularly by the endogenous ligands anandamide or N-arachidonylethanolamine (AEA) and 2-arachidonoylglycerol (2AG) as well as exogenously, by delta-9-tetrahydrocannabinol (THC) and cannabidiol

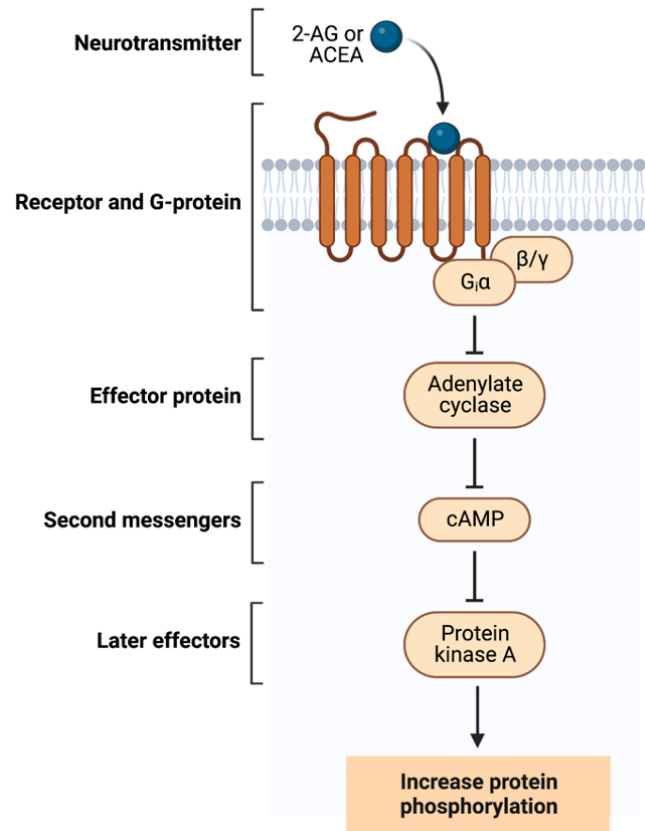


Figure 1.4. CB1R signal transduction pathway increases protein phosphorylation. Figure adapted from “GPCR Effector Pathways” by Biorender.com 2022. Retrieved from <https://app.biorender.com/biorender-templates>

(CBD). The cannabinoid 1 receptor (CB1R) and CB2R can signal through the intracellular calcium pathway (Fan & Yazulla, 2003) or a variety of non-calcium cascades, including by regulating cytoskeletal actin remodeling (Roland et al., 2014).

Studies have demonstrated that cannabis or manipulation of cannabinoid signaling alters the embryonic development of various vertebrate animal models. In the 1960s and 1970s, cannabis injected intraperitoneally or subcutaneously into pregnant rats, guinea pigs, and rabbits during early gestation induced teratogenic effects and congenital malformations in the offspring (Persaud & Ellington, 1968). In more chemically specific experiments, injection of THC or a synthetic ‘herbal spice’ cannabinoid into pregnant mice resulted in increased frequency of cleft palate formation, and malformations in craniofacial complexes, eyes, and brains in fetuses (Bloch et al., 1986; Gilbert et al., 2016). Exposure of gastrula-stage chicken *Gallus gallus* embryos to a water-soluble THC analog resulted in defects in neural tube morphology, head process formation, and expression of neural markers (Psychoyos et al., 2008). In Zebrafish, waterborne exposure to CBD or THC between blastula and larval stages induced eye, snout, and jaw defects, as well as curved axes, tails, and edema (Carty et al., 2018). Finally, the knockdown of the main cannabinoid receptor CB1R in cleavage-stage embryos of *Xenopus laevis* frogs led to smaller, less developed eyes in late tailbud-stage embryos (Zheng et al., 2015). Taken together, these studies demonstrate an impact of cannabis and cannabinoid signaling on neural, craniofacial, and eye morphogenesis (as well as overall body morphology) during embryonic development of various animal models. However, no previous studies, in any developing embryo, have addressed whether CB1R signaling specifically regulates the migration of the cranial neural crest, which is a key embryological

process required for normal craniofacial and eye morphogenesis. In addition, the effects of both activating and inactivating CB1R signaling on craniofacial and eye morphogenesis were not examined in any one type of embryo in these earlier studies. The characterization and accessibility of neural crest migration and craniofacial morphogenesis in non-mammalian vertebrate embryos provide an opportunity to address these questions.

Chapter 2:

Serotonin 2B and 2C receptor disruption leads to cardiac neural crest defects

2.1 Introduction

Currently, many compounds treating the conditions of depression and anxiety target the serotonin 2 family receptors. While the results of many of these treatments, such as psilocybin and MDMA, show incredible therapeutic potential, there is a gap in research regarding the potential teratogenic effects of these compounds. Unfortunately, foundational research needed to infer possible outcomes and indicate the possibility of teratogenicity, specifically regarding the 5-HT receptor activity of these compounds in embryonic development, is also absent.

To address this, we asked whether serotonin receptors 2B and 2C regulate the migration patterns, timing, and differentiation of cardiac neural crest cells. We hypothesized that disrupting the activity at the 5-HT2B and 5-HT2C receptors would result in defects of cNCC migration and derivatives. To test this hypothesis, embryos were treated with 1-Methylpsilocin (1-MP), a specific 5-HT2C agonist and 5-HT2B inverse agonist (Sard et al. 2005). The activity of each receptor was isolated using the specific 5-HT2C antagonist, SB-242084. Effects on cardiac neural crest migration and formation of cardiac neural crest derivatives in the heart were then evaluated at HH30 and HH36.

2.2 Materials and methods

Preparation of pharmacological reagents

A stock solution of 1-Methylpsilocin (1-MP; Tocris Bioscience), an agonist to 5-HT2CR and an inverse agonist to 5-HT2BR, was made in dimethyl sulfoxide (DMSO) to a concentration of 100 mM. A 50 mM stock solution of SB-242084 (SB24; Tocris Bioscience), a highly selective antagonist to 5-HT2CR, was also made in DMSO. The working concentrations for 1-MP and SB-24 were 20 μ M and 10 μ M in Ringer's saline, respectively.

Obtaining and treating embryos

Fertile chicken eggs were obtained from a local farm and incubated in a 1550 Hatcher (GQF Manufacturing) humidified incubator at 37°C for 27-28 hours, to reach stage 8 (HH8; Hamburger and Hamilton, 1951). Working concentrations (20 μ M 1-MP; 10 μ M SB-24) of our test substances were made by dissolving the stock solutions in Howard's Ringer's saline (Ringer's) containing 1:100 penicillin/streptomycin solution. Using an 18-gauge needle, 3 mL of egg white was drawn out of the side of each egg. Next, each egg was opened by cutting a window at the surface of the egg, using sharp stainless-steel scissors (Fine Science Instruments, Item 14060-10). All embryonic treatments consisted of applying 50 μ L of a working concentration of the appropriate reagent onto the dorsal aspect of HH8 embryos, *in ovo*. The stage of the embryo was identified by injecting blue organic food dye diluted in Ringers sub-blastodermally using a 27-gauge ½ inch needle. The eggs were resealed with tape and re-incubated for 22 hours, 6 days, or 10 days, until the embryos reached HH14, HH32, or HH36, respectively. To determine the potential effect of the vehicle, Ringer's control embryos were treated at HH8 with 50 μ L of Ringer's and collected at the same stages.

HH14 embryos were collected onto Whatman paper rings and placed into 1X Phosphate Buffered Solution (PBS). HH32 and HH36 embryos were collected by using a plastic spoon to transfer embryos to 1X PBS wash solutions.

Fixation and Whole Mount Immunohistochemistry

Embryos collected post-treatment at HH14 were fixed for one day at 4°C in 4% paraformaldehyde in PBS, washed 5 times in large volumes of 1X phosphate buffered saline with 0.5% Triton X (PBST), and blocked at 4°C overnight in 1X PBST containing 10% goat serum (blocking solution). HH14 embryos were then double-stained with the primary antibodies Pax7 (pre-migratory and migratory neural crest marker) and HNK1 (migratory neural crest marker). Both primary antibodies were obtained from the Developmental Studies Hybridoma Bank (DSHB) and used at 1:5 dilution in blocking solution, for two days at 4°C. Subsequently, 5 washes with 1x PBST were completed before incubation in secondary antibodies (Alexa fluorophores from Thermofisher Scientific), applied at a 1/500 concentration in blocking buffer, for 1-2 days at 4°C. All embryos were washed extensively in 1x PBST before storage at 4°C and imaging.

Imaging

Embryos were imaged on an upright Zeiss Axio Imager Z1 microscope accessorized with an HPX UV light source and an AxioCamMr3_2 camera run by the software AxioVision Rel.4.8.2.

Reference embryos were imaged using the integrated camera on a Leica S9i digital stereo microscope.

Slides were imaged using an Apple iPhone 11 pro through a compound light microscope.

Paraffin Sectioning

After fixation, HH32 embryos were washed in PBS (6 x 40-min washes and dehydrated in an ascending ethanol series: 60%, 75%, 90%, and 100% (x2 each) for 90 min. Embryos were then transferred to a histological clearing agent, HistoSol (National Diagnostics), for 90 min with two changes. Embryos were infiltrated in a 50% mixture of melted paraffin (Paraplast) and HistoSol for 90 min in an Equatherm vacuum oven (Curtin Matheson Scientific) before being transferred to 100% melted paraffin. Fresh paraffin was added and changed two to three times until no HistoSol remained. Next, the embryos were poured into molds and the resulting blocks were trimmed using a razor blade. A Leitz 1512 microtome was used to section the blocks at 14 μ m and sections were transferred to slides with degassed Millipore water to flatten the tissue onto the slides.

Cryosectioning

Following fixation, HH36 embryos were cut below the cardiac region, and the limbs and head were removed. The samples were then moved into 5% sucrose, 15% sucrose, and 7.5% gelatin sequentially. Samples reached equilibration before being transferred to the next solution. Finally, the samples were placed into molds, covered with an excess of 7.5% gelatin, and frozen at -80°C. Once fully frozen, the embryos were sectioned at 14 μ m on a Microm HM550 cryostat.

Data Analysis

The data analysis program, FIJI (NIH), was used on HH14 embryos to measure the length of the R6NCC stream (**Fig. 2.1C-D, Fig. 2.2D-F**; magenta arrow) and the CirNCC stream (**Fig. 2.1C-D, Fig. 2.2D-F**; gold arrow). The CirNCC length is then divided by the R6NCC length. This ratio is used to evaluate the cardiac neural crest migration pattern at the circumpharyngeal ridge.

Statistical Analysis

All data was stored in Excel spreadsheets. Due to the relatively small sample sizes, the Mann-Whitney U test was used for statistical analysis. A 95% confidence interval was used to determine the statistical significance of the difference.

2.3 Results

Inverse agonism at 5HT2B and agonism at 5HT2C receptors disrupts migration patterns of cNCCs

Control and experimental chick embryos were treated with ringer's saline or 1-MP at HH8, respectively. The embryos were then collected at HH14. By this time, cardiac neural crest migration is in progress, with cardiac crest cells having reached the circumpharyngeal ridge and split into two paths to navigate around the circumpharyngeal ridge. The cNCCs in the rhombomere 6 (R6) stream pause, while the cNCCs that move rostrally (circumpharyngeal neural crest cells) (CirNCC) continue without pausing. This results in a long stream of CirNCCs relative to that of the R6 stream (**Fig. 2.1A**).

Our results show an irregular migration pattern in cNCC streams. In control embryos, patterns in HNK1 expression show that the cNCC migration has reached the circumpharyngeal ridge (**Fig. 2.1B**). In control HH14 embryos, a migration pattern shows a long CirNCC stream with a comparatively short R6NCC stream (ratio mean=2.42; SE=0.33; n=8; **Fig. 2.1C**). In pharmacologically treated embryos, cNCC migration shows an abnormal pattern. In the 1-MP treated embryos, the CirNCC stream has a much similar length to that of the R6NCC stream (ratio

mean=1.323; SE=0.112; n=7; **Fig. 2.1D**). This difference in the ratio of the length of the CirNCC over the length of the R6NCC was found to be statistically significant ($p=0.00412$; **Fig. 2.1E**). These migration anomalies were found to be specific to the cNCC; data analyzing cranial neural crest migration patterns showed no statistically significant difference (data not shown).

Blocking activity at the 5-HT2C receptors does not rescue the cardiac migration phenotype

Rescue experiments were conducted to determine whether 5-HT2B or 5-HT2C or both receptors caused the migration phenotype observed in 1MP-treated embryos. Control embryos were given Ringer's at HH8 and were collected at HH14. To block agonist activity at 5-HT2C, SB242084 (henceforth shortened to SB24), a highly selective 5-HT2C antagonist, was applied to HH14 embryos 10 minutes before the application of Ringer's saline (SB24 embryos) or 1-MP (rescue embryos). The 10-minute wait allows the SB24 to bind and saturate the 5-HT2C receptors and prevent competing with 1-MP. Control embryos displayed a phenotype of a short R6NCC stream compared to a longer CirNCC stream (mean ratio=2.42; SE=0.102; n=8; **Fig. 2.2D**). SB24 followed by Ringer's saline showed no statistically significant difference in the ratio of the R6 stream to the CirNCC stream (mean ratio=1.78; $p=0.189$; SE=0.133; n=7; **Fig. 2.2E**). By contrast, the rescues, exposed to both SB24 and 1-MP, showed a very similar phenotype in the ratio of cNCC stream length that was displayed in the 1-MP treated embryos (mean ratio=1.22; SE=0.0723; n=2; **Fig. 2.2F**). This difference in the ratio of the length of the CirNCC over the length of the R6NCC is distinct from the ratio seen in the control and SB24 embryos.

Inverse agonism at 5HT2B and agonism at 5HT2C receptors induces gaps in the tissue of the aorticopulmonary septum at HH32

To determine whether early phenotypes translate to later ones, or whether a mechanism is activated to recover from early anomalies, embryos were incubated to later stages, when heart septation is underway. CNCC give rise to the aorticopulmonary septum, therefore the aorticopulmonary septum was analyzed on Day 6. Ringer's was applied to control embryos at HH8, and the embryos were collected at HH32 (Embryonic Day 6). In 1-MP embryos, 20 μ M 1-MP was applied to embryos at HH8 and were also collected at HH32. All embryos were then embedded in paraffin and sectioned at 14 μ m. Sections of the heart and the surrounding region were then examined for defects. Heart sections of control embryos collected at HH32 (**Fig. 2.3A**) showed a fully intact aorticopulmonary septum (n=3; **Fig. 2.3B**). In embryos treated with 1-MP at stage HH8, the aorticopulmonary septum displays gaps in the tissue (n=3; **Fig. 2.3C**). These results indicate that the inverse agonism of the 5-HT2B paired with agonism of the 5-HT2C receptor compromises the integrity of tissue of the aorticopulmonary septum.

Defects in the interventricular septum induced by inverse agonism of the 5-HT2B and agonism of the 5-HT2C receptors remain visible at HH36

HH36 embryos were chosen for investigation due to the consistent development of the interventricular septum characteristic at that stage. 1-MP embryos were administered 20 μ M 1-MP at HH8 and were collected at HH36 (Embryonic Day 10). Control embryos were given Ringer's saline at HH8 and were collected at HH36. The collected HH36 embryos (**Fig. 2.4A**) were cryosectioned at 14 μ m with a cryostat after infiltration with gelatin. The resulting sections were examined under a compound light microscope to investigate the development of the

interventricular septum. The control embryos were found to have a fully septated heart with no qualitative difference in gaps between the muscular and cNCC-derived (mesenchymal) septum (n=2; **Fig. 2.4B**). In embryos treated with 1-MP, the interventricular septum is shown to have significant defects. Both of the 1-MP exposed embryos showed more gaps in tissue between the muscular and mesenchymal septum, with one resulting in a large hole (n=2; **Fig. 2.4C**). Together these results suggest that inverse agonism at the 5-HT2B receptor and agonism at the 5-HT2C receptor result in congenital defects of the mesenchymal portion of the interventricular septum.

2.4 Discussion

In this study, using the pharmacological reagents 1-MP and SB24, we showed that inverse agonism activity at the 5-HT2B receptor results in disrupted migration of cNCC at HH14. These results indicate that inverse agonism at the 5-HT2B receptor paired with agonism at the 5-HT2C receptor results in significant gaps in tissue in the aorticopulmonary septum at HH32 and defects of the interventricular septum at HH36.

The mRNA and protein expression of 5-HT2B receptors has been detected in murine embryos in migrating NCCs, neural tube, hematopoietic tissue, and heart primordia by immunohistochemistry and in situ hybridization (Choi et al. 1997). Knockouts performed on the 5-HT2B receptor were observed to perturb myocardial precursor cells and cranial neural crest cells (Choi et al. 1997). A connection could not be drawn between the results found in heart development with altered 5-HT2B activity and cardiac neural crest derivative structures. The results of our study bridge this gap.

The 5-HT_{2C} receptor is also detected in the tissue cNCC derivative structures of murine embryos (Lauder et al. 2000). 5-HT_{2C} knockout mice showed a number of behavioral defects, such as a significant increase in feeding, sleeping, and compulsive behavior (Chou-Greene et al. 2003; Frank et al. 2020). No significant defects in morphology were noted, despite the behavioral abnormalities, suggesting that there may not be a strong link between the 5-HT_{2C} receptor and cardiac development (Frank et al. 2020).

CNCC migration patterns at HH14

As our results show at HH14, disruption of the 5-HT_{2B} receptor as induced by 1-MP alters typical migration patterns of cNCCs (**Fig. 2.1A, D**). At HH14, the R6NCC should have reached the circumpharyngeal ridge, but not continued very far beyond it. This is due to a pause in CirNCC migration while the caudal pharyngeal arches form (Kuratani and Kirby 1992; Kirby and Hutson 2010). While it is known that EphB3/4 are the factors that act as the guidance molecule receptor, it is not currently understood how this pause occurs. It is possible that cardiac crest in embryos with altered 5-HT_{2B} activity fails to pause or does not pause for the same length of time, resulting in the disrupted migration pattern observed (Kuratani and Kirby 1991).

Aorticopulmonary septum defects at HH32

In embryos with inverse agonism at the 5-HT_{2B} receptor, HH32 embryos displayed gaps in the tissue of the aorticopulmonary septum (Fig. 2.3 C). This phenotype is consistent with two possible causes: cardiac fibrosis or apoptosis of cNCCs. Cardiac fibrosis is the build-up of excess extracellular matrix (ECM) components, resulting in fibrous deposits that damage surrounding tissues (Disertori et al. 2017). In embryo sections, this damage manifests as gaps in the tissue.

TGF β 1, a factor that is upregulated downstream of signaling at the 5-HT2B receptor, results in increased fibroblast differentiation (Disertori et al. 2017). Overactivated TGF β 1 signaling led to cardiac fibrosis. While it seems that inverse agonism of the 5-HT2B receptor would induce the opposite, this can only be confirmed by evaluating the ECM of the tissue with altered 5-HT2B intrinsic activity. Future experiments will likely require the use of scanning electron microscopy to confirm this hypothesis, as there is no reliable, universally accepted method for evaluating the components that indicate cardiac fibrosis (de Jong et al. 2012).

An alternative explanation for the gaps in the tissue of the aorticopulmonary septum seen in the 1-MP exposed embryos could be the apoptosis of cNCCs. Apoptosis of cNCCs could be caused by a number of different events but altered timing of migration has been associated with neural crest apoptosis (Choi et al. 1997). Furthermore, the 5-HT2B receptor modulates Bax, a regulator of nuclear apoptosis in murine cardiac tissue (Nebigil and Maroteaux 2003). Future experiments may use *in situ* hybridization chain reaction with probes against Caspase-3/9, an apoptosis marker, to confirm this hypothesis. Cardiac fibrosis can be initiated via apoptosis; cardiac fibrosis can also be a result of apoptosis (Piek et al. 2016). It is currently unknown if perturbing the activity of the 5-HT2B receptor initiates cardiac fibrosis and/or apoptosis.

Interventricular septum defects at HH36

The interventricular septum defect observed in HH36 embryos with disrupted 5-HT2B activity (Fig. 2.4 C) is consistent with interventricular septum defects seen in cNCC ablation experiments (Kirby et al 1985). In the murine model, when antagonists were applied targeting the 5-HT2B receptor, cranial neural crest cells showed disrupted migration and induced apoptosis,

similarly to our results with cNCCs migration of avian embryos. These preliminary results are contingent on an increase of the sample size.

In the future, downregulating 5-HT2B in avian models could provide useful insight into the results shown in this study. In similar studies, modified genetic models and cell labeling has yielded crucial insight into how complex signaling pathways regulate NC function and contribute to cardiac development (Wang et al. 2016). Even though progress has been made in understanding the regulatory networks of NC-derived cardiovascular formation (Erhardt et al. 2021), the developmental processes of NCCs are extraordinarily complex. Further research is required to determine the effect of known contributors at various developmental stages on NC specification, migration, and differentiation, as well as how genetic deficiencies in these pathways lead to congenital heart diseases.

2.6 Figures

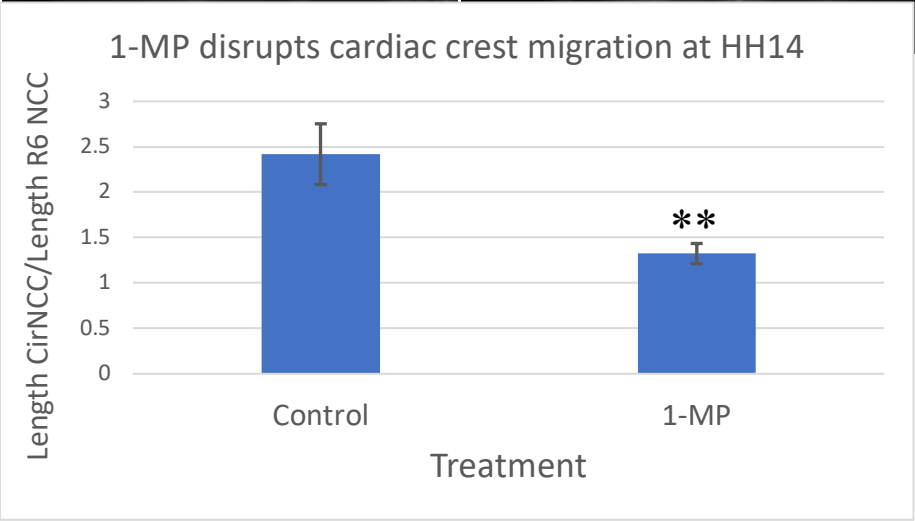
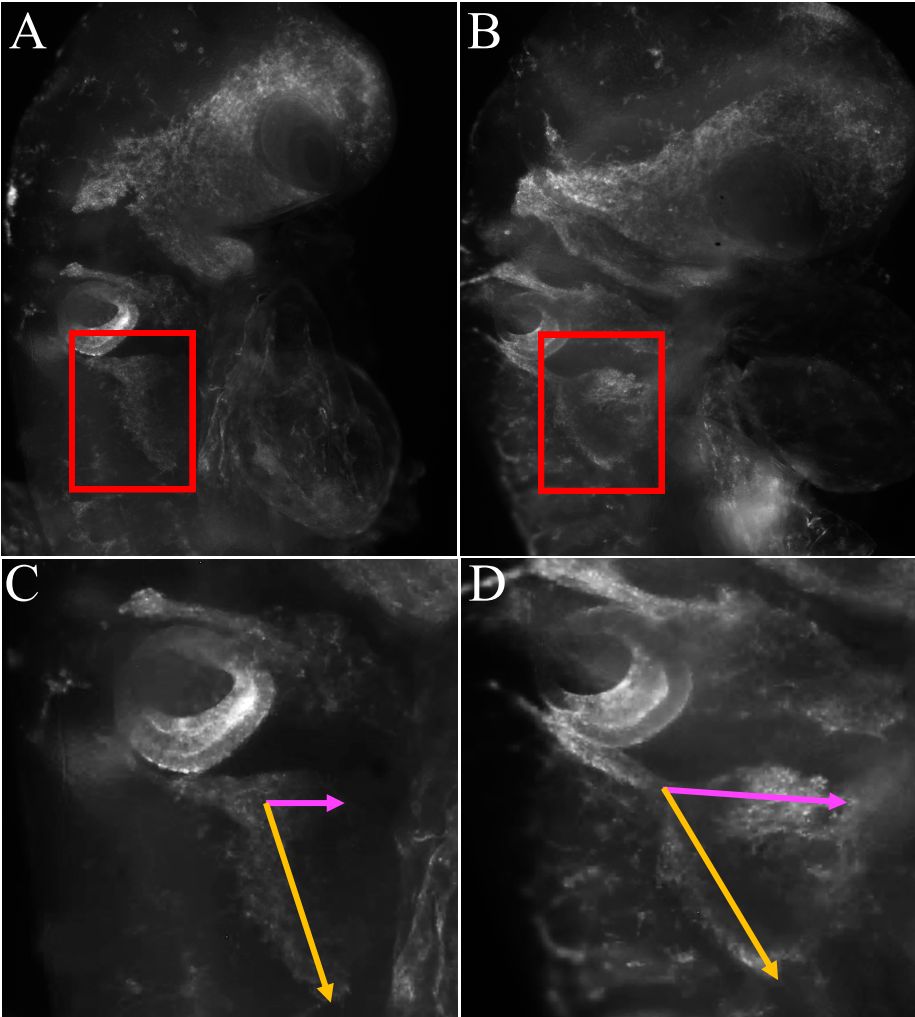


Figure 2.1. 1-MP disrupts the migration patterns of cardiac neural crest in HH14 embryos.

(A) An HH14 control embryo stained with HNK1, a marker of migrating neural crest cells, including cardiac neural crest cells (red box). (B) An HH14 embryo exposed to 20 μ M 1-MP shows HNK1+ cardiac neural crest cells (red box). (C) A close-up image of the control embryo in (A), showing the length of the cardiac neural crest stream at rhombomere 6 (R6NCC) (magenta arrow) as well as the length of the circumpharyngeal neural crest (CirNCC; gold arrow). (D) A close-up image of the cardiac neural crest stream in an HH14 embryo exposed to 20 μ M 1-MP. The R6NCC length (magenta arrow) and the CirNCC length (gold arrow) are similar lengths. (E) The difference in the ratio of R6NCC length to CirNCC length between control and 20 μ M 1-MP treated embryos is statistically significant ($p=0.00412$).

Abbreviations. 1-MP, 1-methylpsilocin; CirNCC, circumpharyngeal neural crest cells; R6NCC, Rhombomere 6 neural crest cells.

** = $p < 0.01$ with a two-tailed Mann-Whitney u-test

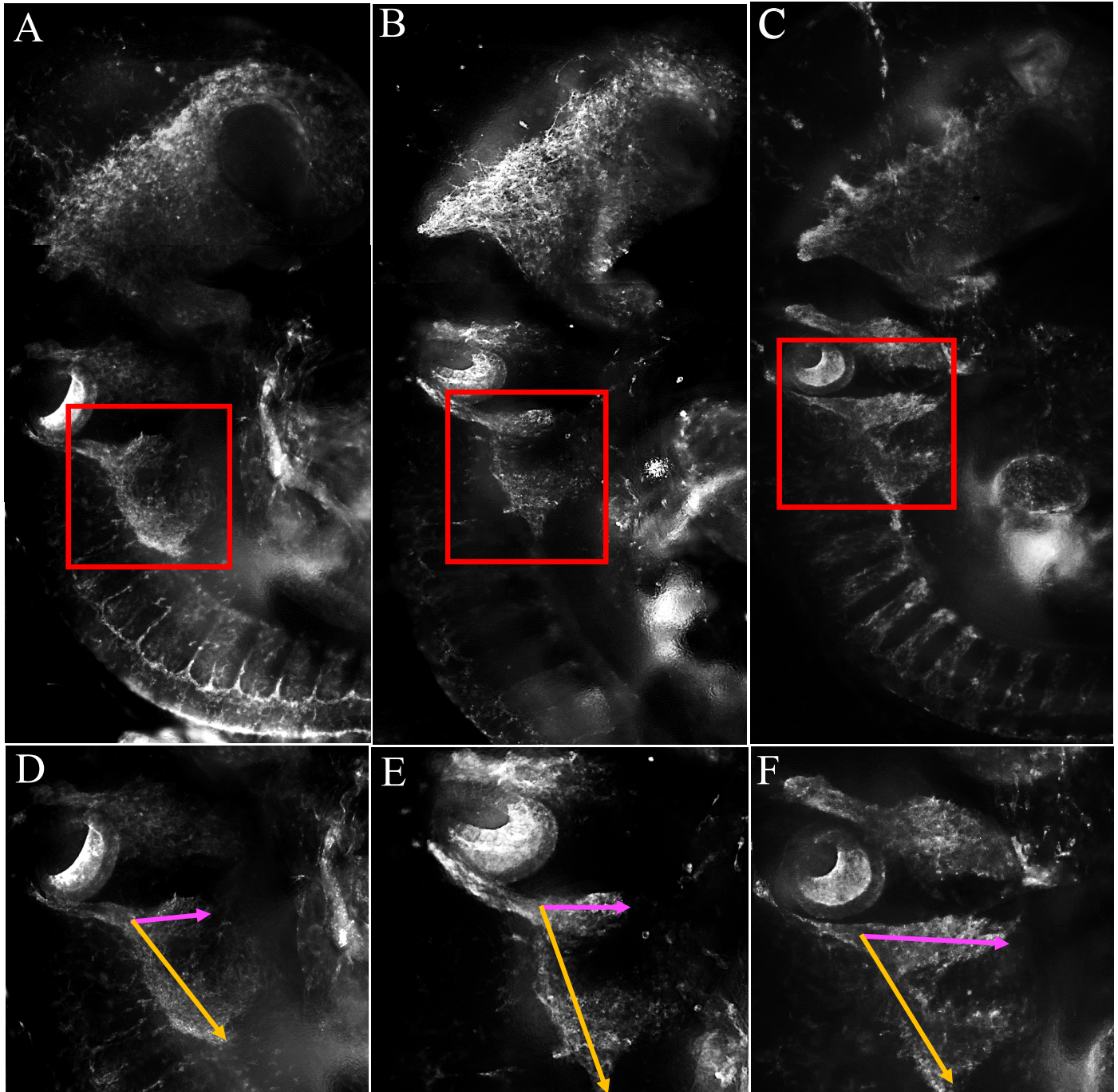


Figure 2.2. Isolating the activity of 5-HT_{2B} does not change the migration defect induced by 1-MP. (A) Migration patterns of cardiac neural crest cells (red box) in a representative HH14 control embryo. (B) An HH14 embryo exposed to 10 μM SB24, with the cardiac neural crest stream shown (red box). (C) The red box delineates cardiac neural crest migrating in a representative HH14 embryo exposed to 10 μM SB24 and to 20 μM 1-MP, after an interval of 10min. (D) A close-up image of the cardiac neural crest in an HH14 control embryo with the rhombomere 6 stream (R6NCC) length (magenta arrow) and circumpharyngeal neural crest stream

(CirNCC) length (gold arrow) (mean ratio=2.42; n=8). **(E)** The magenta arrow depicts the length of the R6NCC stream while the gold arrow denotes the CirNCC length in an HH14 embryo exposed to 20 μ M SB24 (mean ratio=1.78; n=7). **(F)** An HH14 embryo exposed to 10 μ M SB24 and 20 μ M 1-MP with the length measurements for the R6NCC (magenta arrow) and the CirNCC (gold arrow) shown (mean ratio=1.22; n=2)

Abbreviations. 1-MP, 1-methylpsilocin; CirNCC, circumpharyngeal neural crest cells; R6NCC, Rhombomere 6 neural crest cells; SB24, SB-242084.

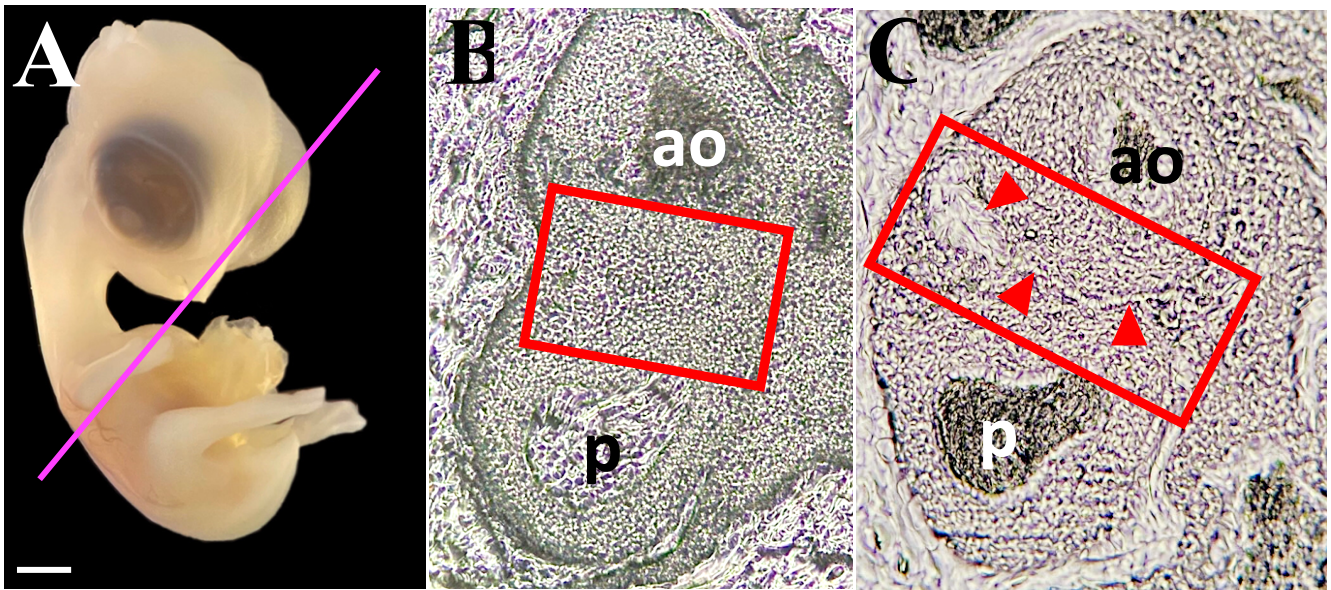


Figure 2.3. 1-MP induces tissue gaps in the aorticopulmonary septum at HH32. (A) An HH32 chick embryo with the orientation of sections (magenta line) for panels B and C. (B) Coronal section through the heart of an HH32 control embryo showing the intact aorticopulmonary septum (red box) between the aorta (ao) and the pulmonary artery (p). (C) The aorticopulmonary septum (red box) displays gaps in the tissue (red arrowheads) in a representative HH32 embryo exposed to 1-MP.

Abbreviations. 1-MP, 1-methylpsilocin; ao, aorta; p, pulmonary artery.

Scale bar 1mm for A

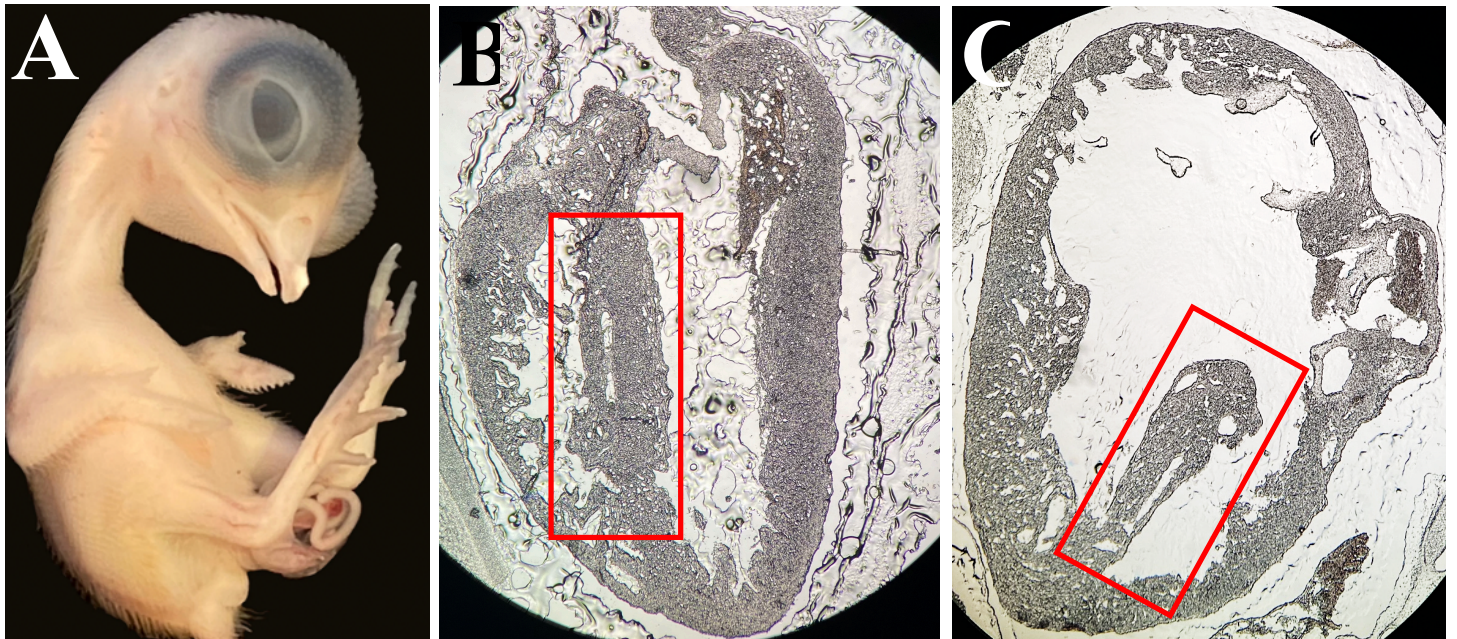


Figure 2.4. 1-MP exposure defects in the interventricular septum at HH36. (A) A representative HH36 chick embryo. Embryos of this stage were sagittally sectioned. Heart sections with this section orientation are shown in panels B and C. (B) A sagittal cryosection of an HH36 control embryo showing the intact interventricular septum (red box). (C) A sagittal cryosection of an HH36 embryo exposed to 1-MP showing an incomplete interventricular septum (red box). Abbreviations. 1-MP, 1-methylpsilocin.

Chapter 3:

Cannabinoid Receptor Type 1 regulates migration and morphogenesis of cranial neural crest

A modified version of this chapter has been submitted for publication as:

Amira Mahomed^{1*}, Daljit Girn^{2*}, Afrin Pattani^{2*}, Brian K. Wells¹, Chloe C. King¹, Christina M. Noravian¹, Jessica Sieminski², Chi Pham², Halley Dante¹, Max Ezin¹, Tamira Elul². Cannabinoid Receptor Type 1 regulates sequential stages of migration and morphogenesis of cranial neural crest and derivatives in chicken and frog embryos.

1. Loyola Marymount University, Department of Biology, Los Angeles CA
2. Touro University California, Basic Sciences Department, College of Osteopathic Medicine, Vallejo, CA

* These authors contributed equally

3.1 INTRODUCTION

In this study, we examined mechanisms for the main cannabinoid receptor, CB1R, in neural crest cell migration and craniofacial and eye morphogenesis in chicken embryos. Previous studies show that the time of onset of expression of CB1R is early (during early neurulation) in chicken embryos (Zheng et al., 2015; Psychoyos et al., 2012; Cottone et al., 2003). Using pharmacological manipulation of CB1R, we show that normal levels of CB1R activity are required for neural crest cell migration and trigeminal ganglion formation in chicken embryos, and craniofacial and eye morphogenesis in frog embryos. Moreover, CB1R mechanisms in these processes are shared by the actin cytoskeleton regulator Myosin II, suggesting that CB1R may signal through an actin regulatory pathway to modulate neural crest migration and craniofacial morphogenesis. Overall, these results imply that all aspects of neural crest development, from emigration to differentiation, are sensitive to manipulation of the endocannabinoid signaling system, in these two organisms that regulate the endocannabinoid system with different timing.

3.2 MATERIALS AND METHODS

Preparation of Pharmacological Reagents

Arachidonyl-2'-chloroethylamide (ACEA), a synthetic agonist of the cannabinoid 1 receptor (CB1R), was obtained from Tocris and speed vacuumed to remove the ethanol solvent. The ethanol was substituted with dimethyl sulfoxide (DMSO) to prepare a 10 mM stock solution. Stock solutions of AM251, a CB1R antagonist (Tocris) and Blebbistatin (Sigma), an inhibitor of

Myosin II ATPase activity, were made by dissolving the reagents in DMSO to a 10 mM concentration.

Obtaining and Treating Embryos

Fertile chicken eggs were obtained from a local farm and incubated at 37°C for 27-28 hours, to reach stage 8 (HH8; Hamburger & Hamilton, 1951). Working concentrations (10 μ M) of our reagents were made by dissolving the stock solutions in Howard's Ringer's saline (Ringer's) containing 1:100 penicillin/streptomycin solution. Using a gauge 18 needle, 3 mL of egg white were drawn out of each egg, from the side, and each egg was opened by cutting a window at the surface of the egg, using sharp stainless-steel scissors (Fine Science Instruments, item 14060-10). All embryonic treatments consisted of applying 50 μ L of a 10 μ M solution of the appropriate reagent onto the dorsal aspect of HH8 embryos, *in ovo*. The eggs were resealed with tape and re-incubated until the embryos reached HH13 or HH18. To determine the potential effect of the vehicle, Ringer's control embryos were treated at HH8 with 50 μ L of Ringer's and collected at HH13. Additional HH13 control embryos were collected without Ringer's pre-treatment. Since the Ringer's control did not result in a different phenotype than the untreated embryos, data from Ringer's controls and untreated controls were pooled. Treatment with ACEA or Blebbistatin essentially did not affect the survival of chick embryos to HH13/14 (75% and 91% survival, respectively) compared to the control embryos, both with (83% survival) and without (58% survival) Ringer's treatment. The same was true for embryo survival to HH18 when treated with ACEA (61%) and AM251 (60%), compared to controls (59%).

Fixation and Antibody Staining

Embryos collected post-treatment at HH13 were fixed for one day at 4°C, washed 5 times in large volumes of 1x phosphate buffered saline (PBS) and blocked at 4°C overnight in 1X PBS containing 0.5% tween, 1% bovine serum albumin, and 10% donkey serum. HH13 embryos were then double-stained with the primary antibodies Pax7 (pre-migratory and migratory neural crest marker) and HNK1 (migratory neural crest marker). Both primary antibodies were obtained from the Developmental Studies Hybridoma Bank (DSHB) and used at 1:5 dilution in block, for two days at 4°C. Subsequently, 5 washes with 1x PBS were completed before incubation in secondary antibodies (Alexa fluorophores from Thermofisher Scientific), applied at a 1/500 concentration in block, for 1-2 days at 4°C. All embryos were washed extensively in 1x PBS before storage at 4°C and imaging.

Immunohistochemistry with HH18 embryos followed the procedure detailed above with the difference that the primary antibody used to detect gangliogenesis was TUJ1 (marker of neuronal cell body and axon; Covance) dissolved 1:300 in block.

Imaging

A Zeiss Stemi 305 microscope was used to examine and mount HH13 and HH14 embryos on slides, such that the brain vesicles of each embryo could be seen. HH18 embryos were plated on their right and left sides to image both trigeminal ganglia. An upright, Zeiss Axio Imager Z1 microscope accessorized with a HPX UV light source and an AxioCamMr3_2 camera, was used to image each embryo using the software AxioVision Rel.4.8.2.

Data Analysis

Chicken Embryos Stage 13/14

The FIJI software (NIH) was used to trace the border of the midbrain and the midbrain neural crest cells (HNK1-positive) of HH13 embryos. From these perimeters, the respective areas were computed. The ratio of midbrain neural crest cell area (**Fig. 3.1A**, orange dashes) to midbrain area (**Fig 3.1A**; green tracing) was calculated in control and ACEA-treated embryos. In HH14 embryos, the width of the embryonic head and the width of the field of migratory neural crest cells (characterized by HNK1 expression) were measured with FIJI software. The extent of the migrating neural crest cells was assessed using the following method: (a) a vertical line was drawn starting from the forming mandible using the posterior eye as a reference point (**Fig. 3.1B**, orange arrow); (b) for consistency, the shortest line was drawn from that point on the mandible to the top of the HNK1 field (**Fig. 3.1B**, green arrow); (c) the same angle and reference point was used to extend a line from the mandible to the top of the head (**Fig. 3.1B**, sum of pink arrow and green arrow). The value from (b) was then divided by the value from (c) for control, ACEA- and Blebbistatin-treated embryos. These ratios were used to evaluate the proportion of head space occupied by migratory neural crest cells.

Chicken Embryos Stage 18

For morphometric analysis of the trigeminal ganglia at HH18, the area, perimeter, and circularity (shape) of each trigeminal ganglion in control, ACEA- and AM251-treated embryos were measured. The area, perimeter, circularity, and length of the ganglion's maxillomandibular and ophthalmic lobes, with their associated nerves, were also measured (**Fig. 3.2A**). All measurements were taken separately on the right and left sides of each embryo.

Statistical Analysis

All data was stored in Excel spreadsheets. Due to the relatively small sample sizes, the Mann-Whitney U test was used for statistical analysis. A 95% confidence interval was used to determine the statistical significance of the difference.

3.3 RESULTS

Over-activating CB1R reduces dispersion of cranial neural crest cells in midbrain of chicken embryos

To determine whether CB1R plays a role in the migratory behaviors of neural crest cells, chicken embryos were treated with arachidonyl-2'-chloroethylamide (ACEA), a CB1R agonist, at HH8. At this stage, neural crest cells have not started migrating and are still found at the dorsal aspect of the neural tube (Kulesa & Fraser, 1998; Kulesa et al., 2010). As cranial neural crest cells migrate, they disperse over the midbrain. Control embryos were either exposed to Ringer's (vehicle) or left untreated. Because both Ringer's and untreated groups gave similar results, these embryos were pooled and will be referred to as "controls" from this point. To observe neural crest migration after treatment, embryos were re-incubated until HH13, when cranial neural crest migration is in progress. Neural crest migration was assessed by normalizing HNK1-positive domain (neural crest domain) area to total midbrain area at HH13 (**Fig. 3.1A**).

Cranial neural crest cells in pharmacologically treated embryos dispersed differently in the midbrain than they did in control embryos. In ACEA-treated embryos (n = 11), dramatically fewer HNK1-positive cells were seen migrating atop the midbrain, compared to the number of

cells found in control embryos ($n = 12$; **Fig. 3.1B, C**). Furthermore, the neural crest cells present in ACEA-treated embryos were collected in one area of the midbrain (yellow outline); this smaller distribution was reflected in a relatively small ratio of midbrain neural crest cell area (yellow tracing) to total midbrain area (green tracing; average ratio 0.38; SE = 0.032; $p < 0.05$; **Fig. 3.1D**). By contrast, midbrain neural crest in controls occupied almost the entirety of the midbrain area (yellow outline; average ratio 0.79; SE = 0.10). In brief, overactivation of signaling through CB1R inhibited cranial neural crest cells from spreading across the midbrain, as in control embryos.

CB1R agonism and perturbation of Myosin II oppositely modulate cranial neural crest migration in chicken embryos

The abnormal distribution of neural crest cells at the midbrain in HH13 chicken embryos treated with the CB1R agonist prompted us to investigate the impact of this disturbance on longer range neural crest migration. As neural crest cells migrate, they remodel their actin cytoskeleton by altering Myosin II activity (Berndt et al., 2008). Accordingly, we also performed experiments in which we treated HH8 embryos with Blebbistatin, a non-muscle Myosin II ATPase inhibitor that interferes with actin-dependent motility (Straight et al., 2003). Embryos were treated at pre-migratory neural crest stage 8 and collected at HH14, when embryo turning offers a profile view of the head with neural crest cells having reached and accumulated at the edges of the forming jaw. We obtained a normalized migratory crest distance by calculating the ratio of width of HNK1 expression domain (**Fig. 3.2A**, green arrow; **Fig. 3.2 B-D**, yellow arrows) to total head width (**Fig. Fig. 3.2A**, sum of green plus pink arrows; **Fig. 3.2 B-D**, green arrows), from a point on the jaw caudal to the eye (**Fig. 3.2A**, orange arrow).

Both overactivation of CB1R with ACEA and inhibition of actomyosin interactions with Blebbistatin disturbed cranial neural crest migration patterns in HH14 embryos. In controls, the accumulation of the migratory neural crest cells at a greater distance from the midbrain resulted in a width of the HNK1 expression domain (**Fig. 3.2B**, yellow arrow) with an average ratio 0.49 (SE = 0.014; n = 8; **Fig. 3.2E**). By contrast, in embryos exposed to ACEA (n = 8), the HNK1 domain occupied a significantly smaller portion of the head (average ratio 0.44; SE = 0.029; $p < 0.05$; **Fig. 3.2C**, yellow arrow; **Fig. 3.2E**). Also reaching statistical significance, the larger width of the HNK1 field in embryos exposed to Blebbistatin (0.61; SE: 0.026; $p < 0.0001$; n = 17) showed that cranial neural crest migration was decreased compared to controls (**Fig. 3.2D**, yellow arrow; **Fig. 3.2E**).

These results support the notion that both overactivation of CB1R and inhibition of non-muscle myosin II perturb migratory behaviors in cranial neural crest cells.

Over-activation and inactivation of CB1R disrupts trigeminal ganglion development in chicken embryos

Neural crest cells are precursors of the peripheral nervous system; as such, they contribute to all cranial nerves (Le Douarin & Smith, 1988). Since migration of the cranial neural crest was dysregulated following over-activation of CB1R, we asked whether the derivatives of those neural crest cells might also be affected. The largest sensory cranial nerve - the trigeminal ganglion (**Fig. 3.2A**) - was examined at HH18 in chick embryos. Furthermore, to determine the potential effect of imbalance in CB1R signaling, in addition to over-activating CB1R in a test group with the agonist ACEA, we inhibited signaling through that receptor by applying the antagonist AM251.

Initial inspection and analysis showed that ACEA treatment decreased, whereas AM251 application increased, the proportion of the trigeminal ganglia displaying ophthalmic and maxillomandibular nerves (**Fig. 3.2A**). 40% of ACEA-treated embryos (n = 20 ganglia in 10 embryos) and 94% of AM251-treated embryos (n = 18 ganglia in 9 embryos) displayed an ophthalmic nerve, compared to 80% of controls (n = 30 ganglia in 15 embryos; **Fig. 3.2C, D**). Similarly, whereas 60% of maxillomandibular lobes in control embryos showed the beginning of axon formation, 40% (n = 20 ganglia) and 83% (n = 18 ganglia) of maxillomandibular lobes displayed nerve formation in ACEA and AM251-treated embryos, respectively.

Morphometric analysis expanded our understanding of these phenotypic differences between experimental and control trigeminal ganglia and showed that they stemmed from morphological changes occurring specifically on the right side of the embryo. The mean length, perimeter, and area of the right-side ophthalmic lobe and its nerve were significantly smaller, and the mean circularity was significantly larger (indicating a rounder shape), in ACEA-exposed embryos than the same measurements from right ophthalmic lobes and nerves in controls (**Fig. 3.2F-I, Table 1**). In AM251-treated embryos, the right-side ophthalmic lobe and its nerve were significantly longer and its circularity significantly smaller (denoting a less round shape) than control ophthalmic lobes with nerves; however, the area and perimeter of the AM251 right-side ophthalmic lobe with nerve were similar to controls (**Fig. 3.2F, Table 1**). Similarly, the length of the right-side maxillomandibular lobe with nerve was significantly shorter in the ACEA group than in the control group (**Fig. 3.2F, Table 1**). However, in AM251-exposed embryos, all right-side maxillomandibular parameters (area, length, perimeter, circularity) were similar to controls (**Fig. 3.2F-I, Table 1**).

As these measurements included both the lobes and the nerves of the trigeminal ganglia, the phenotypes could be due to differences between lobes rather than nerves. To confirm that these phenotypes were due to changes in the ophthalmic and maxillomandibular nerve projection and not in lobes, we also measured parameters for the lobes of the ganglia specifically, without their nerves. This analysis showed that in ACEA- and AM251-treated embryos, the length, perimeter, area, and circularity of the lobes were statistically similar to controls ($p < 0.05$ for all measurements).

In brief, our data suggest that over-activation and inactivation of signaling through CB1R oppositely modulate ophthalmic and maxillomandibular nerve formation in the trigeminal ganglion. In addition, a discrepancy was observed between the right and left sides, as all left-side trigeminal parameters were comparable to controls, with both pharmacological treatments.

3.4 DISCUSSION

Using pharmacological reagents, we show that normal signaling activity of the main cannabinoid receptor, CB1R, is required for neural crest migration and trigeminal ganglion formation in chicken embryos. The effects of disrupting CB1R signaling on neural crest migration were mimicked by the inhibition of non-muscle Myosin II. These findings suggest that cannabinoid signaling is required for sequential stages in neural crest migration and morphogenesis in chicken embryos. Our results also imply that CB1R signals through Myosin II to regulate neural crest migration. Experiments not detailed here and carried out in frog embryos by our collaborators at Touro University showed that cranial neural crest derivatives are similarly impacted by the disruption of cannabinoid receptor, CB1R, or non-muscle myosin II.

Cannabinoid Receptor Type 1 impacts neural crest migration and trigeminal ganglion formation in chicken embryos

Results presented here suggest that CB1R signaling is required for normal migration of cranial neural crest cells in chicken embryos. Following application of a CB1R pharmacological activator, ACEA, cranial neural crest cells in the midbrain of chick embryos migrated erratically, in smaller numbers and in clumps. In contrast, in controls, large numbers of neural crest cells migrated individually across the full area of the midbrain. The clumped, restricted distribution of neural crest cells with overactivated cannabinoid signaling suggests that CB1R may normally regulate cell-to-cell adhesion between neural crest cells, and thereby crest migration. This is the first study to demonstrate that cannabinoid signaling is required for migration of neural crest cells in any type of embryo *in vivo*. Accordingly, this defines a novel function for CB1R in a significant cellular process during an intermediate developmental stage of embryogenesis. Although no previous studies have shown that cannabinoid signaling is required for neural crest migration, reports demonstrated that cannabinoid signaling regulates migration of cells during earlier embryonic developmental stages. Tight regulation of cannabinoid signaling was required for spiral artery trophoblast giant cells to appropriately invade the maternal mesometrial pole during placentation (Xie et al. 2012). CB1R has also been shown to modulate cell motility and morphology in pathological contexts. In cultured glioblastoma cells, cannabinoids caused an abnormal distribution of actin cytoskeletal elements and, as a result, an abnormal cell shape (Hohmann et al. 2019). Overactivation of the endocannabinoid signaling also suppressed the migration of metastatic breast cancer cells (Qamri et al. 2009).

The formation of the trigeminal ganglion and nerve requires epithelial-to-mesenchymal transition, migration, condensation, neuronal differentiation, and mixing and adhesion of both trigeminal placode cells and cranial neural crest cells (Shiau et al. 2008). Those processes, and their underlying molecular regulations (Wu & Taneyhill 2019; Gammill et al. 2006; McCabe et al. 2009; Simon et al. 2017), seem to be relatively undisturbed in ACEA- and AM251-treated embryos, since the trigeminal ganglia do form (**Fig. 3.2**) and their lobes show normal morphometric parameters (perimeter, area, length and circularity). Moreover, expression of the neuronal marker Tuj1 by the trigeminal ganglia suggests that differentiation is not impacted by disruption of the cannabinoid pathway. These results support the notion that the endocannabinoid system does not play a role in gangliogenesis.

However, overactivation of CB1R with ACEA prevented, or at least delayed, nerve projection in the majority of ophthalmic lobes of the trigeminal ganglia in chick embryos, as evidenced by a shorter ophthalmic lobe with nerve. This result is reminiscent of the aberrant nerve projection from the optic nerve in frog embryos treated with ACEA (Elul et al. 2022) or disoriented axonal processes from cortical neurons in the mouse and the Rhesus monkey (Morozov et al. 2020). AM251 treatment caused the trigeminal nerve to form more posteriorly than expected, closer to the otic pit. This hints at a caudal displacement of the trigeminal placode, a key player in trigeminal morphogenesis (Shiau et al. 2008). As a result of this caudal slippage, the ophthalmic nerve projected to the eye at a more acute angle, accounting for the smaller circularity value. It is noteworthy that the ophthalmic nerve did reach the eye region by HH18, suggesting that axonal extension may have occurred at an increased rate in AM251, to bridge the larger distance to the eye in the same amount of time as controls. Furthermore, AM251 ophthalmic nerve was often overly defasciculated, showing mistargeted axons (**Fig. 3.2E**). Supporting our *in vivo* results,

another group showed that explanted trigeminal ganglia exposed to AM251 had mistargeted axons that turned back to innervate the midbrain (Watson et al. 2008). Lastly, the maxillomandibular lobe and nerve in trigeminal ganglia was generally less affected than its ophthalmic counterpart, likely because nerve formation has not progressed very far by HH18.

Interestingly, there seems to be a right-left discrepancy in our results, with the ophthalmic or maxillomandibular lobes on the right side of the embryo being affected, while near-normal development occurs on the left side, with both pharmacological treatments. Although we are unclear about the possible left-right mechanism, we note that CB1R expression displays a left-right asymmetric expression in gastrulating chick embryos in the node (Psychoyos et al. 2012) by HH8, and this may underpin the later differences in right versus left ganglionic nerve morphogenesis.

CB1R impacts later cranial crest derivatives: submitted data using frog embryos.

Later derivatives of the cranial neural crest include craniofacial bones, in addition to cranial nerves. The frog model system offers fast access to high numbers of embryos that develop quickly to later stages. Therefore, we collaborated with the Elul lab, to study late craniofacial effects of manipulating CB1R signaling. The later onset of CB1R expression in frog, as compared to chick (Elul et al. 2022) further solidified our lens on late morphogenesis.

The Elul lab demonstrated that signaling of cannabinoid type 1 receptor, CB1R, influences and is required for normal craniofacial and eye morphogenesis in tailbud stage embryos of *Xenopus laevis* frogs. Both pharmacological activation and inactivation of CB1R signaling led to smaller, misshapen, and less developed craniofacial complexes and eye regions in frog embryos. These findings confirm and extend the results of earlier studies that examined the impacts of

cannabis and manipulation of cannabinoid signaling on development of craniofacial and eye regions in embryos of other species. In very early studies, cannabis injection into pregnant rabbits, rats, and guinea pigs, resulted in altered craniofacial and eye regions of the developing fetuses (Persaud & Ellington, 1968). In later studies, ingestion of THC or a synthetic ‘herbal spice’ cannabinoid by pregnant mice induced craniofacial and eye defects in mouse fetuses, such as micrognathia (small jaws) and facial clefts, as well as microphthalmia (smaller eyes), iridial coloboma and anophthalmia (lack of eyes; Bloch et al., 1986; Gilbert et al., 2016). In addition, in zebrafish, waterborne exposure of animals to CBD and THC led to eye and snout defects (Carty et al., 2018). Finally, knockdown of the CB1R receptor in *Xenopus laevis* cleavage stage embryos resulted in reduced eyes at late tailbud stages (Zheng et al., 2015). Extending from these studies, our results are the first to show that both activation and inactivation of the cannabinoid receptor, CB1R, induce similar craniofacial and eye defects in one type of embryo. This suggests that tight homeostatic regulation of CB1R is required for normal craniofacial and eye morphogenesis in developing frog embryos.

Myosin II exerts shared mechanisms with CB1R in regulation of cranial neural crest migration and craniofacial and eye morphogenesis

Blebbistatin, a non-muscle Myosin II inhibitor, was used to treat chick embryos, while our collaborators similarly treated frog tadpoles. The application of Blebbistatin, a non-muscle Myosin II inhibitor, impacted cranial neural crest cell migration in an opposite manner to ACEA, the CB1R agonist. By HH14, in embryos exposed to ACEA or Blebbistatin, cranial neural crest cells had migrated significantly less far than their counterparts in control embryos. In addition, craniofacial and eye morphogenesis were similarly impacted by Blebbistatin as by both the CB1R activator

ACEA and inactivator AM251. Treatment with Blebbistatin resulted in smaller and misshapen craniofacial regions and reduced eye regions as did ACEA and AM251. Together, these results suggest that signaling of cannabinoids through CB1R may regulate activity of non-muscle Myosin II to modulate neural crest migration from the neural tube in chicken embryos and migratory or morphogenetic processes of neural crest derivatives that are required for craniofacial and eye morphogenesis in frog embryos. Other researchers have shown that CB1R, a G-protein coupled receptor, signals through ROCK and Rho to regulate Myosin II activity in growth cone motility of a developing neuronal circuit (Roland et al., 2014). A similar molecular mechanism may be involved in CB1R regulation of Myosin II to promote neural crest and derivative migration and morphogenesis in chicken and frog embryos.

3.5 CONCLUSIONS

We show that in chicken embryos, sequential steps of neural crest cell migration and differentiation are perturbed by alterations in cannabinoid signaling. The time of onset of expression of CB1R is significantly earlier in chick (*Gallus gallus*, during neurulation) than in frog embryos (*Xenopus laevis*, at early tailbud stage). Accordingly, our results suggest that CB1R impacts the migration and morphogenesis of neural crest cells and neural crest derivatives through all developmental stages, in different classes of animals. This data advances our understanding of the functions of cannabinoid signaling on neural crest migration and differentiation of neural crest-derived structures during embryonic development.

3.6 Figures

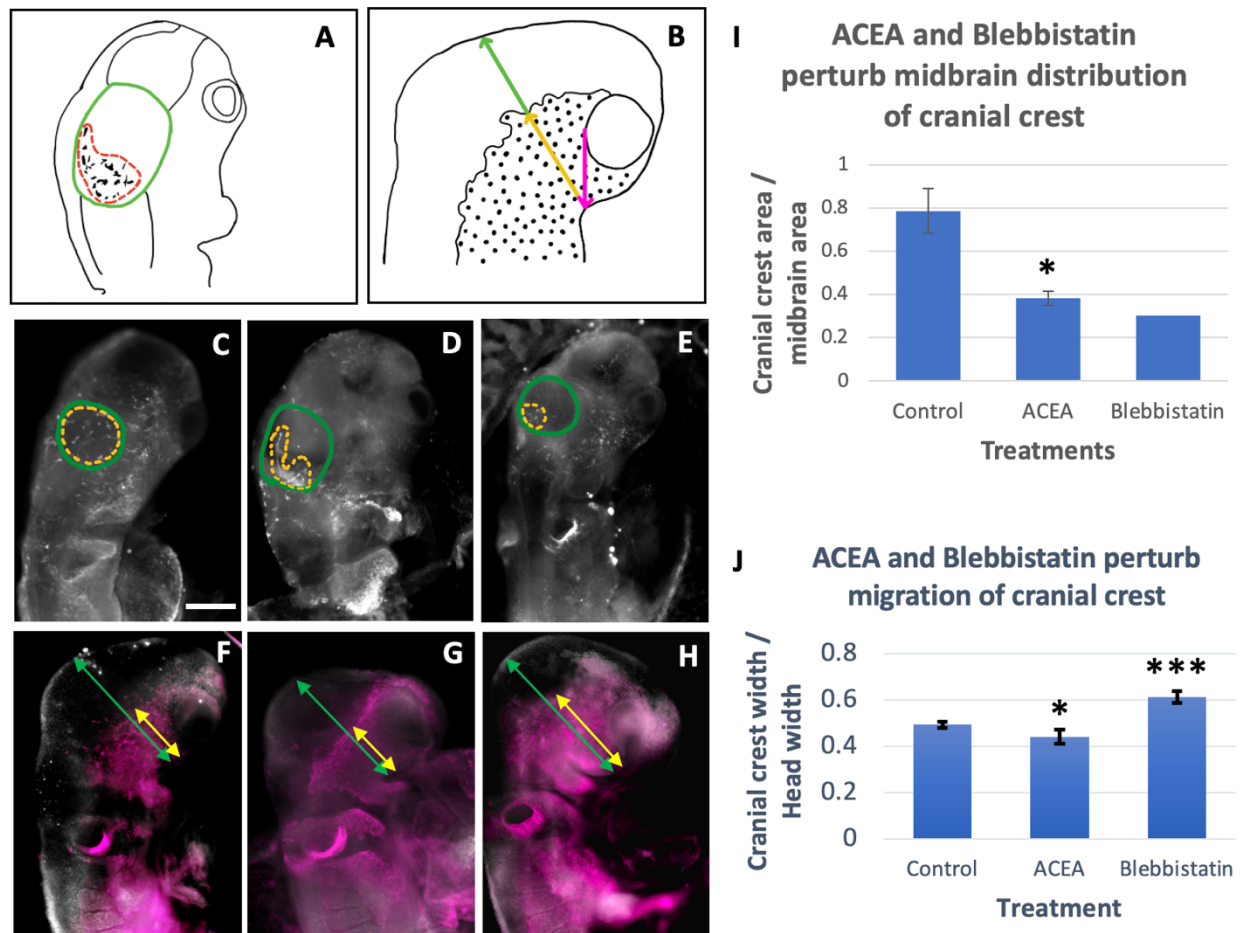


Figure 3.1. CB1R overactivation and myosin II inhibition perturb cranial neural crest cell migration in chick embryos. (A) HH13: Method for assessing the distribution (orange dashes) of cranial neural crest cells (speckles) in the midbrain (green outline). (B) HH14: Method for quantifying the extent the migration (yellow arrow) of cranial neural crest cells (speckles), caudal to the eye (pink arrow) and as a proportion of the width of the head (combined length of green and yellow arrows). (C) HH13 control embryo with a large area of HNK1 expression (yellow circle) relative to the midbrain area (green circle). (D) An HH13 embryo exposed to ACEA shows a small HNK1 domain (yellow tracing) relative to the midbrain (green circle). (E) In Blebbistatin-treated embryos, cranial neural crest cells (HNK1 expression) occupy a small area (yellow circle) in the midbrain (green circle) at HH13. (F) HH14 control embryo shows a standard width of HNK1 expression (yellow arrow) relative to the head width (green arrow). (G) Neural crest cells in embryos treated with ACEA extend over a smaller width at HH14 (HNK1 expression; yellow arrow). (H) HH14 embryo exposed to Blebbistatin, with a wide HNK1 domain (yellow arrow) in proportion to the head (green arrow). (I) ACEA significantly impacts the distribution of neural crest cells in the midbrain. (J) ACEA and myosin II inhibition affect the ratio of the width of HNK1 domain to width of head.

* p < 0.05; *** p < 0.001. Scale bar 0.3 mm for C-H.

Table 3.1. Statistically significant measurements of the right ophthalmic and maxillo-mandibular lobes with respective nerves.

Lobe and nerve	Treatment (number of lobes with nerve, number of embryos)	Length SE (μm)	Perimeter SE (μm)	Area SE (μm^2)	Circularity SE
Right ophthalmic lobe and nerve	Control (15, 15)	760 60.0	1,834 140.7	71,382 4,949.0	0.3 0.041
	ACEA (10, 10)	500 * 84.3	1,155 * 170.6	45,209 * 6,275.7	0.5 * 0.070
	AM251 (9, 9)	1,024 * 76.6	-	-	0.2 * 0.019
Right maxillo-mandibular lobe and nerve	Control (15, 15)	492 32.0	-	-	-
	ACEA (10, 10)	383 * 29.0	-	-	-
	AM251 (9, 9)	-	-	-	-

* p < 0.05

Data not shown was not statistically different from controls.

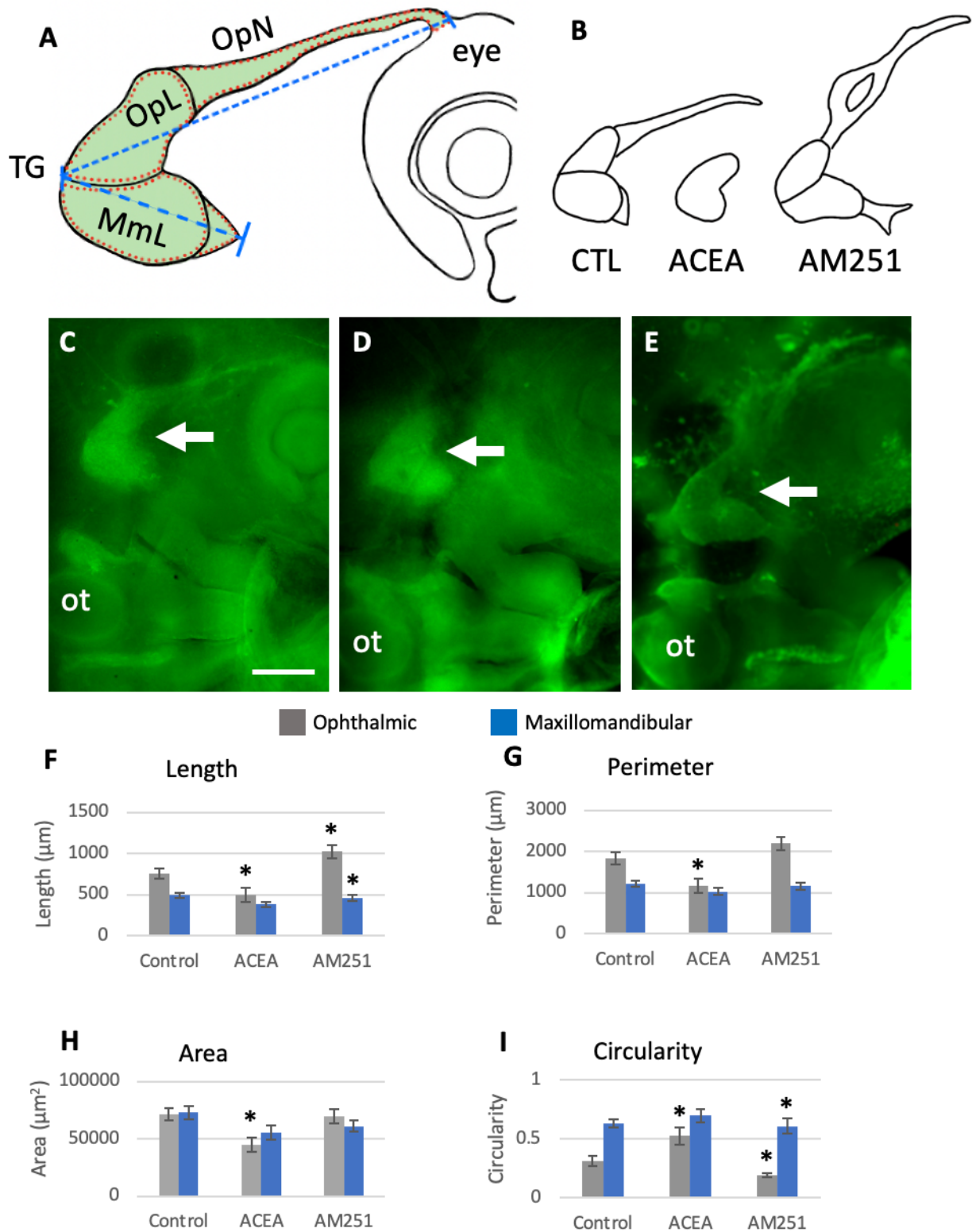


Figure 3.2. Trigeminal ganglion phenotypes vary with treatments in HH18 Embryos. (A) Method for measuring parameters. Green color = area. Blue line = length. Red dots = perimeter. **(B) Tracings of right trigeminal nerves** reveal phenotypic differences resulting from different treatment conditions. Control ganglia consistently extend the ophthalmic nerve. ACEA-treated

trigeminal ganglia are smaller than control ganglia and regularly lack the ophthalmic nerve. AM251-treated ganglia are positioned more posteriorly, often show defasciculation of the ophthalmic nerve and a high angle between the ophthalmic nerve and the eye. **(C)** Control embryo with ophthalmic nerve (arrow) to eye. Asterisk denotes the otic vesicle. **(D)** ACEA-treated embryos lacking ophthalmic nerve. **(E)** AM251-treated embryo with increased angle of the ophthalmic nerve projecting to the eye. **(F)** Graph showing the area of the right ophthalmic and maxillomandibular lobes with nerves for each treatment. **(G)** Data for the length of the right ophthalmic and maxillomandibular lobes with nerves. **(H)** Perimeter of the right ophthalmic and maxillomandibular lobes with nerves. **(I)** Circularity of ophthalmic and maxillomandibular lobes with nerves.

* $p < 0.05$. Scale bar 0.3 mm for C-E.

Abbreviations. Ctl, Control; MmL, Maxillomandibular lobe; OpL, Ophthalmic lobe; OpN, Ophthalmic nerve; Ot, otic vesicle; TG, Trigeminal ganglion.

Chapter 4:

Discussion

The study of neurotransmitters has been well investigated in adults; however, their role as humoral morphogens is often overlooked. In the future, I hope to continue my exploration of the impacts of neurotransmitters in embryonic development. The use of genetic tools such as knockdowns/ knockouts and constitutive activation of specific receptors paired with single-cell RNA seq can relatively easily illuminate downstream effects as a result of increased or decreased receptor activation (Qian et al. 2017).

It is possible that the findings of this study could inform therapies that target the 2 family serotonin receptors. 4-phosphorloxy-N,N-dimethyltryptamine (psilocybin) is a naturally occurring psychedelic compound being studied in conjunction with psychotherapy for treating several psychiatric diseases. Psilocybin has a relatively low binding affinity and intrinsic activity at serotonin receptors until dephosphorylated by alkaline diphosphatase into 4-hydroxy-N,N-dimethyltryptamine (psilocin). Psilocin is the bioactive metabolite of psilocybin that causes *in vivo* psychedelic activity in humans and animals (e.g., head twitch response) through agonist activities at the 2 family 5-HT receptors, namely the 5-HT_{2B} receptor (Collins et al. 1966). Treatments using psilocybin have shown therapeutic promise (Griffiths et al. 2016) but are understudied as they pertain to embryonic development.

Compounds targeting the endocannabinoid system have become a focus of both medicinal and recreational applications. The compound delta-9-tetrahydrocannabinol (THC) is a partial agonist at the cannabinoid 1 and 2 receptors. THC consumption has greatly increased as a result of legalization and due to studies suggesting that THC has a wide possibility of medicinal treatments, such as cancer-related pain (Johnson et al. 2010). Cannabidiol (CBD), a compound

with observed anxiolytic and painkilling effects (Kwee et al. 2022; Donvito et al. 2018), acts as an antagonist to cannabinoid receptors 1 and 2 (Pertwee 2008) and as an agonist to the serotonin 1A receptor (Martinez-Aguirre et al. 2020). The findings of this study could provide some foundational knowledge to inform of possible teratogenic effects of these treatments and call for further investigation.

References

- Almogi-Hazan, O., & Or, R. (2020). Cannabis, the Endocannabinoid System and Immunity—The Journey from the Bedside to the Bench and Back. *International Journal of Molecular Sciences*, 21(12), 4448. <https://doi.org/10.3390/ijms21124448>
- Arif, Y., Singh, P., Bajguz, A., & Hayat, S. (2021). Phytocannabinoids Biosynthesis in Angiosperms, Fungi, and Liverworts and Their Versatile Role. *Plants*, 10(7), 1307. <https://doi.org/10.3390/plants10071307>
- Berndt, J. D., Clay, M. R., Langenberg, T., & Halloran, M. C. (2008). Rho-kinase and myosin II affect dynamic neural crest cell behaviors during epithelial to mesenchymal transition in vivo. *Developmental Biology*, 324(2), 236–244. <https://doi.org/10.1016/j.ydbio.2008.09.013>
- Bloch, E., Fishman, R. H. B., Morrill, G. A., & Fujimoto, G. I. (1986). The effect of intragastric administration of Δ^9 -tetrahydrocannabinol on the growth and development of fetal mice of the AJ strain. *Toxicology and Applied Pharmacology*, 82(2), 378–382. [https://doi.org/10.1016/0041-008X\(86\)90215-2](https://doi.org/10.1016/0041-008X(86)90215-2)
- Bockman, D. E., Redmond, M. E., & Kirby, M. L. (1989). Alteration of early vascular development after ablation of cranial neural crest. *The Anatomical Record*, 225(3), 209–217. <https://doi.org/10.1002/ar.1092250306>
- Bookman, D. E., Redmond, M. E., Waldo, K., Davis, H., & Kirby, M. L. (1987). Effect of neural crest ablation on development of the heart and arch arteries in the chick. *American Journal of Anatomy*, 180(4), 332–341. <https://doi.org/10.1002/aja.1001800403>
- Braun, M., Wunderlin, M., Spieth, K., Knöchel, W., Gierschik, P., & Moepps, B. (2002). Xenopus laevis Stromal cell-derived factor 1: Conservation of structure and function during vertebrate

development. *Journal of Immunology (Baltimore, Md.: 1950)*, 168(5), 2340–2347.

<https://doi.org/10.4049/jimmunol.168.5.2340>

Britsch, S., Goerich, D. E., Riethmacher, D., Peirano, R. I., Rossner, M., Nave, K.-A., Birchmeier, C., & Wegner, M. (2001). The transcription factor Sox10 is a key regulator of peripheral glial development. *Genes & Development*, 15(1), 66–78. <https://doi.org/10.1101/gad.186601>

Bronner, M. E. (2012). Formation and migration of neural crest cells in the vertebrate embryo.

Histochemistry and Cell Biology, 138(2), 179–186. <https://doi.org/10.1007/s00418-012-0999-z>

Bryan, C. D., Casey, M. A., Pfeiffer, R. L., Jones, B. W., & Kwan, K. M. (2020). Optic cup morphogenesis requires neural crest-mediated basement membrane assembly. *Development*, dev.181420. <https://doi.org/10.1242/dev.181420>

Buznikov, G. A., Lambert, W. H., & Lauder, J. M. (2001). Serotonin and serotonin-like substances as regulators of early embryogenesis and morphogenesis. *Cell and Tissue Research*, 305(2), 177–186. <https://doi.org/10.1007/s004410100408>

Callén, L., Moreno, E., Barroso-Chinea, P., Moreno-Delgado, D., Cortés, A., Mallol, J., Casadó, V., Lanciego, J. L., Franco, R., Lluís, C., Canela, E. I., & McCormick, P. J. (2012). Cannabinoid Receptors CB1 and CB2 Form Functional Heteromers in Brain. *Journal of Biological Chemistry*, 287(25), 20851–20865. <https://doi.org/10.1074/jbc.M111.335273>

Carmona-Fontaine, C., Matthews, H. K., Kuriyama, S., Moreno, M., Dunn, G. A., Parsons, M., Stern, C. D., & Mayor, R. (2008). Contact inhibition of locomotion in vivo controls neural crest directional migration. *Nature*, 456(7224), 957–961. <https://doi.org/10.1038/nature07441>

Carty, D. R., Thornton, C., Gledhill, J. H., & Willett, K. L. (2018). Developmental Effects of Cannabidiol and Δ^9 -Tetrahydrocannabinol in Zebrafish. *Toxicological Sciences*, 162(1), 137–145. <https://doi.org/10.1093/toxsci/kfx232>

- Chang, C.-J., Chao, C.-H., Xia, W., Yang, J.-Y., Xiong, Y., Li, C.-W., Yu, W.-H., Rehman, S. K., Hsu, J. L., Lee, H.-H., Liu, M., Chen, C.-T., Yu, D., & Hung, M.-C. (2011). P53 regulates epithelial–mesenchymal transition and stem cell properties through modulating miRNAs. *Nature Cell Biology*, 13(3), 317–323. <https://doi.org/10.1038/ncb2173>
- Cheung, M., Chaboissier, M.-C., Mynett, A., Hirst, E., Schedl, A., & Briscoe, J. (2005). The Transcriptional Control of Trunk Neural Crest Induction, Survival, and Delamination. *Developmental Cell*, 8(2), 179–192. <https://doi.org/10.1016/j.devcel.2004.12.010>
- Choi, D. S., Ward, S. J., Messaddeq, N., Launay, J. M., & Maroteaux, L. (1997). 5-HT_{2B} receptor-mediated serotonin morphogenetic functions in mouse cranial neural crest and myocardial cells. *Development*, 124(9), 1745–1755. <https://doi.org/10.1242/dev.124.9.1745>
- Collins, R. L., Ordy, J. M., & Samorajski, T. (1966). Psilocin: Effects on Behaviour and Brain Serotonin in Mice. *Nature*, 209(5025), Article 5025. <https://doi.org/10.1038/209785a0>
- Conway, S. J., Godt, R. E., Hatcher, C. J., Leatherbury, L., Zolotouchnikov, V. V., Brotto, M. A. P., Copp, A. J., Kirby, M. L., & Creazzo, T. L. (1997). Neural Crest is Involved in Development of Abnormal Myocardial Function. *Journal of Molecular and Cellular Cardiology*, 29(10), 2675–2685. <https://doi.org/10.1006/jmcc.1997.0499>
- Creazzo, T. L. (1990). Reduced L-type calcium current in the embryonic chick heart with persistent truncus arteriosus. *Circulation Research*, 66(6), 1491–1498. <https://doi.org/10.1161/01.RES.66.6.1491>
- Creazzo, T. L., Brotto, M. A. P., & Burch, J. (1997). Excitation-Contraction Coupling in the Day 15 Embryonic Chick Heart with Persistent Truncus Arteriosus. *Pediatric Research*, 42(6), 731–737. <https://doi.org/10.1203/00006450-199712000-00002>

- Dady, A., Blavet, C., & Duband, J.-L. (2012). Timing and kinetics of E- to N-cadherin switch during neurulation in the avian embryo. *Developmental Dynamics*, 241(8), 1333–1349.
<https://doi.org/10.1002/dvdy.23813>
- Dash, S., & Trainor, P. A. (2020). The development, patterning and evolution of neural crest cell differentiation into cartilage and bone. *Bone*, 137, 115409.
<https://doi.org/10.1016/j.bone.2020.115409>
- de Jong, S., van Veen, T. A. B., de Bakker, J. M. T., & van Rijen, H. V. M. (2012). Monitoring cardiac fibrosis: A technical challenge. *Netherlands Heart Journal*, 20(1), 44–48.
<https://doi.org/10.1007/s12471-011-0226-x>
- Disertori, M., Masè, M., & Ravelli, F. (2017). Myocardial fibrosis predicts ventricular tachyarrhythmias. *Trends in Cardiovascular Medicine*, 27(5), 363–372.
<https://doi.org/10.1016/j.tcm.2017.01.011>
- Dottori, M., Gross, M. K., Labosky, P., & Goulding, M. (2001). The winged-helix transcription factor Foxd3 suppresses interneuron differentiation and promotes neural crest cell fate. *Development (Cambridge, England)*, 128(21), 4127–4138. <https://doi.org/10.1242/dev.128.21.4127>
- Duband, J.-L. (2010). Diversity in the molecular and cellular strategies of epithelium-to-mesenchyme transitions: Insights from the neural crest. *Cell Adhesion & Migration*, 4(3), 458–482.
<https://doi.org/10.4161/cam.4.3.12501>
- Elul, T., Lim, J., Hanton, K., Lui, A., Jones, K., Chen, G., Chong, C., Dao, S., & Rawat, R. (2022). Cannabinoid Receptor Type 1 regulates growth cone filopodia and axon dispersion in the optic tract of *Xenopus laevis* tadpoles. *European Journal of Neuroscience*, 55(4), 989–1001.
<https://doi.org/10.1111/ejn.15603>

- Erhardt, S., Zheng, M., Zhao, X., Le, T. P., Findley, T. O., & Wang, J. (2021). The Cardiac Neural Crest Cells in Heart Development and Congenital Heart Defects. *Journal of Cardiovascular Development and Disease*, 8(8), 89. <https://doi.org/10.3390/jcdd8080089>
- Fonseca, B. M., Correia-da-Silva, G., Taylor, A. H., Konje, J. C., Bell, S. C., & Teixeira, N. A. (2009). Spatio-temporal expression patterns of anandamide-binding receptors in rat implantation sites: Evidence for a role of the endocannabinoid system during the period of placental development. *Reproductive Biology and Endocrinology*, 7(1), 121. <https://doi.org/10.1186/1477-7827-7-121>
- Frank, M. G., Stryker, M. P., & Tecott, L. H. (2002). Sleep and Sleep Homeostasis in Mice Lacking the 5-HT_{2c} Receptor. *Neuropsychopharmacology : Official Publication of the American College of Neuropsychopharmacology*, 27(5), 869–873. [https://doi.org/10.1016/S0893-133X\(02\)00353-6](https://doi.org/10.1016/S0893-133X(02)00353-6)
- Gammill, L. S., Gonzalez, C., & Bronner-Fraser, M. (2007). Neuropilin 2/semaphorin 3F signaling is essential for cranial neural crest migration and trigeminal ganglion condensation. *Developmental Neurobiology*, 67(1), 47–56. <https://doi.org/10.1002/dneu.20326>
- George, R. M., Maldonado-Velez, G., & Firulli, A. B. (2020). The heart of the neural crest: Cardiac neural crest cells in development and regeneration. *Development*, 147(20), dev188706. <https://doi.org/10.1242/dev.188706>
- Gilbert, M. T., Sulik, K. K., Fish, E. W., Baker, L. K., Dehart, D. B., & Parnell, S. E. (2016). Dose-dependent teratogenicity of the synthetic cannabinoid CP-55,940 in mice. *Neurotoxicology and Teratology*, 58, 15–22. <https://doi.org/10.1016/j.ntt.2015.12.004>
- Griffiths, R. R., Johnson, M. W., Carducci, M. A., Umbricht, A., Richards, W. A., Richards, B. D., Cosimano, M. P., & Klinedinst, M. A. (2016). Psilocybin produces substantial and sustained decreases in depression and anxiety in patients with life-threatening cancer: A randomized

double-blind trial. *Journal of Psychopharmacology (Oxford, England)*, 30(12), 1181–1197.

<https://doi.org/10.1177/0269881116675513>

Gülck, T., & Møller, B. L. (2020). Phytocannabinoids: Origins and Biosynthesis. *Trends in Plant Science*, 25(10), 985–1004. <https://doi.org/10.1016/j.tplants.2020.05.005>

Hamblet, N. S., Lijam, N., Ruiz-Lozano, P., Wang, J., Yang, Y., Luo, Z., Mei, L., Chien, K. R., Sussman, D. J., & Wynshaw-Boris, A. (2002). Dishevelled 2 is essential for cardiac outflow tract development, somite segmentation and neural tube closure. *Development*, 129(24), 5827–5838.

<https://doi.org/10.1242/dev.00164>

Hamburger, V., & Hamilton, H. L. (1992). A series of normal stages in the development of the chick embryo. *Developmental Dynamics*, 195(4), 231–272. <https://doi.org/10.1002/aja.1001950404>

Hohmann, T., Feese, K., Ghadban, C., Dehghani, F., & Grabiec, U. (2019). On the influence of cannabinoids on cell morphology and motility of glioblastoma cells. *PLOS ONE*, 14(2), e0212037. <https://doi.org/10.1371/journal.pone.0212037>

Huang, G. Y., Cooper, E. S., Waldo, K., Kirby, M. L., Gilula, N. B., & Lo, C. W. (1998). Gap Junction-mediated Cell-Cell Communication Modulates Mouse Neural Crest Migration. *Journal of Cell Biology*, 143(6), 1725–1734. <https://doi.org/10.1083/jcb.143.6.1725>

Hutson, M. R., & Kirby, M. L. (2003). Neural crest and cardiovascular development: A 20-year perspective. *Birth Defects Research Part C: Embryo Today: Reviews*, 69(1), 2–13.

<https://doi.org/10.1002/bdrc.10002>

Hutson, M. R., Zhang, P., Stadt, H. A., Sato, A. K., Li, Y.-X., Burch, J., Creazzo, T. L., & Kirby, M. L. (2006). Cardiac arterial pole alignment is sensitive to FGF8 signaling in the pharynx.

Developmental Biology, 295(2), 486–497. <https://doi.org/10.1016/j.ydbio.2006.02.052>

- Jain, R., Engleka, K. A., Rentschler, S. L., Manderfield, L. J., Li, L., Yuan, L., & Epstein, J. A. (2011). Cardiac neural crest orchestrates remodeling and functional maturation of mouse semilunar valves. *The Journal of Clinical Investigation*, *121*(1), 422–430.
<https://doi.org/10.1172/JCI44244>
- Jenkins, T., Nguyen, J., Polglaze, K., & Bertrand, P. (2016). Influence of Tryptophan and Serotonin on Mood and Cognition with a Possible Role of the Gut-Brain Axis. *Nutrients*, *8*(1), 56.
<https://doi.org/10.3390/nu8010056>
- Johnson, J. R., Burnell-Nugent, M., Lossignol, D., Ganae-Motan, E. D., Potts, R., & Fallon, M. T. (2010). Multicenter, Double-Blind, Randomized, Placebo-Controlled, Parallel-Group Study of the Efficacy, Safety, and Tolerability of THC:CBD Extract and THC Extract in Patients with Intractable Cancer-Related Pain. *Journal of Pain and Symptom Management*, *39*(2), 167–179.
<https://doi.org/10.1016/j.jpainsymman.2009.06.008>
- Kirby, M. L. (1987). Cardiac Morphogenesis—Recent Research Advances. *Pediatric Research*, *21*(3), Article 3. <https://doi.org/10.1203/00006450-198703000-00001>
- Kirby, M. L., & Creazzo, T. L. (1995). Cardiovascular Development: Neural Crest and New Perspectives. *Cardiology in Review*, *3*(4), 226. <https://doi.org/10.1097/00045415-199507000-00006>
- Kirby, M. L., & Hutson, M. R. (2010). Factors controlling cardiac neural crest cell migration. *Cell Adhesion & Migration*, *4*(4), 609–621. <https://doi.org/10.4161/cam.4.4.13489>
- Kirby, M. L., Turnage, K. L., & Hays, B. M. (1985). Characterization of conotruncal malformations following ablation of “cardiac” neural crest. *The Anatomical Record*, *213*(1), 87–93.
<https://doi.org/10.1002/ar.1092130112>

- Kirby, M. L., & Waldo, K. L. (1990). Role of neural crest in congenital heart disease. *Circulation*, 82(2), 332–340. <https://doi.org/10.1161/01.CIR.82.2.332>
- Kirby, M. L., & Waldo, K. L. (1995). Neural Crest and Cardiovascular Patterning. *Circulation Research*, 77(2), 211–215. <https://doi.org/10.1161/01.RES.77.2.211>
- Kontges, G., & Lumsden, A. (1996). Rhombencephalic neural crest segmentation is preserved throughout craniofacial ontogeny. *Development*, 122(10), 3229–3242. <https://doi.org/10.1242/dev.122.10.3229>
- Krispin, S., Nitzan, E., Kassem, Y., & Kalcheim, C. (2010). Evidence for a dynamic spatiotemporal fate map and early fate restrictions of premigratory avian neural crest. *Development*, 137(4), 585–595. <https://doi.org/10.1242/dev.041509>
- Kruk-Slomka, M., Dzik, A., Budzynska, B., & Biala, G. (2017). Endocannabinoid System: The Direct and Indirect Involvement in the Memory and Learning Processes—a Short Review. *Molecular Neurobiology*, 54(10), 8332–8347. <https://doi.org/10.1007/s12035-016-0313-5>
- Kulesa, P., Ellies, D. L., & Trainor, P. A. (2004). Comparative analysis of neural crest cell death, migration, and function during vertebrate embryogenesis. *Developmental Dynamics*, 229(1), 14–29. <https://doi.org/10.1002/dvdy.10485>
- Kulesa, P. M., Bailey, C. M., Kasemeier-Kulesa, J. C., & McLennan, R. (2010). Cranial neural crest migration: New rules for an old road. *Developmental Biology*, 344(2), 543–554. <https://doi.org/10.1016/j.ydbio.2010.04.010>
- Kulesa, P. M., & Fraser, S. E. (1998). Neural Crest Cell Dynamics Revealed by Time-Lapse Video Microscopy of Whole Embryo Chick Explant Cultures. *Developmental Biology*, 204(2), 327–344. <https://doi.org/10.1006/dbio.1998.9082>

- Kuratani, S. C., & Kirby, M. L. (1991). Initial migration and distribution of the cardiac neural crest in the avian embryo: An introduction to the concept of the circumpharyngeal crest. *The American Journal of Anatomy*, 191(3), 215–227. <https://doi.org/10.1002/aja.1001910302>
- Kuratani, S. C., & Kirby, M. L. (1992). Migration and distribution of circumpharyngeal crest cells in the chick embryo. Formation of the circumpharyngeal ridge and E/C8+ crest cells in the vertebrate head region. *The Anatomical Record*, 234(2), 263–280. <https://doi.org/10.1002/ar.1092340213>
- Kwee, C. M., van Gerven, J. M., Bongaerts, F. L., Cath, D. C., Jacobs, G., Baas, J. M., & Groenink, L. (2022). Cannabidiol in clinical and preclinical anxiety research. A systematic review into concentration–effect relations using the IB-de-risk tool. *Journal of Psychopharmacology (Oxford, England)*, 36(12), 1299–1314. <https://doi.org/10.1177/02698811221124792>
- Lauder, J. M., Wilkie, M. B., Wu, C., & Singh, S. (2000). Expression of 5-HT(2A), 5-HT(2B) and 5-HT(2C) receptors in the mouse embryo. *International Journal of Developmental Neuroscience: The Official Journal of the International Society for Developmental Neuroscience*, 18(7), 653–662. [https://doi.org/10.1016/s0736-5748\(00\)00032-0](https://doi.org/10.1016/s0736-5748(00)00032-0)
- Lauder, J. M., & Zimmerman, E. F. (1988). Sites of serotonin uptake in epithelia of the developing mouse palate, oral cavity, and face: Possible role in morphogenesis. *Journal of Craniofacial Genetics and Developmental Biology*, 8(3), 265–276.
- Le Douarin, N. M., & Smith, J. (1988). Development of the Peripheral Nervous System from the Neural Crest. *Annual Review of Cell Biology*, 4(1), 375–404. <https://doi.org/10.1146/annurev.cb.04.110188.002111>

- Leatherbury, L., Gauldin, H. E., Waldo, K., & Kirby, M. L. (1990). Microcinematography of the developing heart in neural crest-ablated chick embryos. *Circulation*, *81*(3), 1047–1057. <https://doi.org/10.1161/01.CIR.81.3.1047>
- Li, Y., Gonzalez, W. G., Andreev, A., Tang, W., Gandhi, S., Cunha, A., Prober, D., Lois, C., & Bronner, M. E. (2020). Macropinocytosis-mediated membrane recycling drives neural crest migration by delivering F-actin to the lamellipodium. *Proceedings of the National Academy of Sciences*, *117*(44), 27400–27411. <https://doi.org/10.1073/pnas.2007229117>
- Lumsden, A., Sprawson, N., & Graham, A. (1991). Segmental origin and migration of neural crest cells in the hindbrain region of the chick embryo. *Development*, *113*(4), 1281–1291. <https://doi.org/10.1242/dev.113.4.1281>
- Luo, Y., High, F. A., Epstein, J. A., & Radice, G. L. (2006). N-cadherin is required for neural crest remodeling of the cardiac outflow tract. *Developmental Biology*, *299*(2), 517–528. <https://doi.org/10.1016/j.ydbio.2006.09.003>
- Mackie, K. (2005). Cannabinoid receptor homo- and heterodimerization. *Life Sciences*, *77*(14), 1667–1673. <https://doi.org/10.1016/j.lfs.2005.05.011>
- Mani, S. A., Guo, W., Liao, M.-J., Eaton, E. Ng., Ayyanan, A., Zhou, A. Y., Brooks, M., Reinhard, F., Zhang, C. C., Shipitsin, M., Campbell, L. L., Polyak, K., Briskin, C., Yang, J., & Weinberg, R. A. (2008). The Epithelial-Mesenchymal Transition Generates Cells with Properties of Stem Cells. *Cell*, *133*(4), 704–715. <https://doi.org/10.1016/j.cell.2008.03.027>
- Martínez-Aguirre, C., Carmona-Cruz, F., Velasco, A. L., Velasco, F., Aguado-Carrillo, G., Cuéllar-Herrera, M., & Rocha, L. (2020). Cannabidiol Acts at 5-HT1A Receptors in the Human Brain: Relevance for Treating Temporal Lobe Epilepsy. *Frontiers in Behavioral Neuroscience*, *14*. <https://www.frontiersin.org/articles/10.3389/fnbeh.2020.611278>

- Mathews, J., & Levin, M. (2017). Gap junctional signaling in pattern regulation: Physiological network connectivity instructs growth and form. *Developmental Neurobiology*, 77(5), 643–673. <https://doi.org/10.1002/dneu.22405>
- Mayor, R., & Theveneau, E. (2013). The neural crest. *Development*, 140(11), 2247–2251. <https://doi.org/10.1242/dev.091751>
- McCabe, K. L., Sechrist, J. W., & Bronner-Fraser, M. (2009). Birth of ophthalmic trigeminal neurons initiates early in the placodal ectoderm. *The Journal of Comparative Neurology*, 514(2), 161–173. <https://doi.org/10.1002/cne.22004>
- McCusker, C., Cousin, H., Neuner, R., & Alfandari, D. (2009). Extracellular Cleavage of Cadherin-11 by ADAM Metalloproteases Is Essential for *Xenopus* Cranial Neural Crest Cell Migration. *Molecular Biology of the Cell*, 20(1), 78–89. <https://doi.org/10.1091/mbc.e08-05-0535>
- McKeown, S. J., Wallace, A. S., & Anderson, R. B. (2013). Expression and function of cell adhesion molecules during neural crest migration. *Developmental Biology*, 373(2), 244–257. <https://doi.org/10.1016/j.ydbio.2012.10.028>
- McKinney, M. C., Fukatsu, K., Morrison, J., McLennan, R., Bronner, M. E., & Kulesa, P. M. (2013). Evidence for dynamic rearrangements but lack of fate or position restrictions in premigratory avian trunk neural crest. *Development*, 140(4), 820–830. <https://doi.org/10.1242/dev.083725>
- McKinney, M. C., Stark, D. A., Teddy, J., & Kulesa, P. M. (2011). Neural crest cell communication involves an exchange of cytoplasmic material through cellular bridges revealed by photoconversion of KikGR. *Developmental Dynamics*, 240(6), 1391–1401. <https://doi.org/10.1002/dvdy.22612>
- McLennan, R., Schumacher, L. J., Morrison, J. A., Teddy, J. M., Ridenour, D. A., Box, A. C., Semerad, C. L., Li, H., McDowell, W., Kay, D., Maini, P. K., Baker, R. E., & Kulesa, P. M.

- (2015). Neural crest migration is driven by a few trailblazer cells with a unique molecular signature narrowly confined to the invasive front. *Development*, 142(11), 2014–2025.
<https://doi.org/10.1242/dev.117507>
- McPartland, J. M., Matias, I., Di Marzo, V., & Glass, M. (2006). Evolutionary origins of the endocannabinoid system. *Gene*, 370, 64–74. <https://doi.org/10.1016/j.gene.2005.11.004>
- Milet, C., & Monsoro-Burq, A. H. (2012). Neural crest induction at the neural plate border in vertebrates. *Developmental Biology*, 366(1), 22–33. <https://doi.org/10.1016/j.ydbio.2012.01.013>
- Moiseiwitsch, J. R., & Lauder, J. M. (1995). Serotonin regulates mouse cranial neural crest migration. *Proceedings of the National Academy of Sciences of the United States of America*, 92(16), 7182–7186.
- Morel, A.-P., Lièvre, M., Thomas, C., Hinkal, G., Ansieau, S., & Puisieux, A. (2008). Generation of Breast Cancer Stem Cells through Epithelial-Mesenchymal Transition. *PLoS ONE*, 3(8), e2888.
<https://doi.org/10.1371/journal.pone.0002888>
- Morozov, Y. M., Mackie, K., & Rakic, P. (2020). Cannabinoid Type 1 Receptor is Undetectable in Rodent and Primate Cerebral Neural Stem Cells but Participates in Radial Neuronal Migration. *International Journal of Molecular Sciences*, 21(22), 8657.
<https://doi.org/10.3390/ijms21228657>
- Nakamura, T., Colbert, M. C., & Robbins, J. (2006). Neural Crest Cells Retain Multipotential Characteristics in the Developing Valves and Label the Cardiac Conduction System. *Circulation Research*, 98(12), 1547–1554. <https://doi.org/10.1161/01.RES.0000227505.19472.69>
- Nandadasa, S., Tao, Q., Menon, N. R., Heasman, J., & Wylie, C. (2009). N- and E-cadherins in *Xenopus* are specifically required in the neural and non-neural ectoderm, respectively, for F-actin

assembly and morphogenetic movements. *Development*, 136(8), 1327–1338.

<https://doi.org/10.1242/dev.031203>

Nebigil, C. G., & Maroteaux, L. (2003). Functional Consequence of Serotonin/5-HT_{2B} Receptor Signaling in Heart. *Circulation*, 108(7), 902–908.

<https://doi.org/10.1161/01.CIR.0000081520.25714.D9>

Nichols, D. H. (1986). Formation and distribution of neural crest mesenchyme to the first pharyngeal arch region of the mouse embryo. *American Journal of Anatomy*, 176(2), 221–231.

<https://doi.org/10.1002/aja.1001760210>

Oltrabella, F., Melgoza, A., Nguyen, B., & Guo, S. (2017). Role of the endocannabinoid system in vertebrates: Emphasis on the zebrafish model. *Development, Growth & Differentiation*, 59(4), 194–210. <https://doi.org/10.1111/dgd.12351>

Osumi-Yamashita, N., Ninomiya, Y., Eto, K., & Doi, H. (1994). The contribution of both forebrain and midbrain crest cells to the mesenchyme in the frontonasal mass of mouse embryos. *Developmental Biology*, 164(2), 409–419. <https://doi.org/10.1006/dbio.1994.1211>

Perez-Alcala, S., Nieto, M. A., & Barbas, J. A. (2004). LSox5 regulates RhoB expression in the neural tube and promotes generation of the neural crest. *Development*, 131(18), 4455–4465. <https://doi.org/10.1242/dev.01329>

Persaud, T. V. N., & Ellington, A. C. (1968). Teratogenic activity of cannabis resin. *The Lancet*, 292(7564), 406–407. [https://doi.org/10.1016/S0140-6736\(68\)90626-0](https://doi.org/10.1016/S0140-6736(68)90626-0)

Pertwee, R. G. (2008). The diverse CB₁ and CB₂ receptor pharmacology of three plant cannabinoids: Δ^9 -tetrahydrocannabinol, cannabidiol and Δ^9 -tetrahydrocannabivarin. *British Journal of Pharmacology*, 153(2), 199–215. <https://doi.org/10.1038/sj.bjp.0707442>

- Piacentino, M. L., Li, Y., & Bronner, M. E. (2020). Epithelial-to-mesenchymal transition and different migration strategies as viewed from the neural crest. *Current Opinion in Cell Biology*, 66, 43–50. <https://doi.org/10.1016/j.ceb.2020.05.001>
- Piek, A., de Boer, R. A., & Silljé, H. H. W. (2016). The fibrosis-cell death axis in heart failure. *Heart Failure Reviews*, 21(2), 199–211. <https://doi.org/10.1007/s10741-016-9536-9>
- Prasad, M. S., Sauka-Spengler, T., & LaBonne, C. (2012). Induction of the neural crest state: Control of stem cell attributes by gene regulatory, post-transcriptional and epigenetic interactions. *Developmental Biology*, 366(1), 10–21. <https://doi.org/10.1016/j.ydbio.2012.03.014>
- Pryor, S. E., Massa, V., Savery, D., Andre, P., Yang, Y., Greene, N. D. E., & Copp, A. J. (2014). Vangl-dependent planar cell polarity signalling is not required for neural crest migration in mammals. *Development*, 141(16), 3153–3158. <https://doi.org/10.1242/dev.111427>
- Psychoyos, D., Vinod, K. Y., Cao, J., Xie, S., Hyson, R. L., Wlodarczyk, B., He, W., Cooper, T. B., Hungund, B. L., & Finnell, R. H. (2012). Cannabinoid Receptor 1 Signaling in Embryo Neurodevelopment: CB1 signaling in embryo neurodevelopment. *Birth Defects Research Part B: Developmental and Reproductive Toxicology*, 95(2), 137–150. <https://doi.org/10.1002/bdrb.20348>
- Qamri, Z., Preet, A., Nasser, M. W., Bass, C. E., Leone, G., Barsky, S. H., & Ganju, R. K. (2009). Synthetic cannabinoid receptor agonists inhibit tumor growth and metastasis of breast cancer. *Molecular Cancer Therapeutics*, 8(11), 3117–3129. <https://doi.org/10.1158/1535-7163.MCT-09-0448>
- Qian, Y., Cao, Y., Deng, B., Yang, G., Li, J., Xu, R., zhang, D., Huang, J., & Rao, Y. (n.d.). Sleep homeostasis regulated by 5HT2b receptor in a small subset of neurons in the dorsal fan-shaped body of drosophila. *ELife*, 6, e26519. <https://doi.org/10.7554/eLife.26519>

- Rinon, A., Molchadsky, A., Nathan, E., Yovel, G., Rotter, V., Sarig, R., & Tzahor, E. (2011). P53 coordinates cranial neural crest cell growth and epithelial-mesenchymal transition/delamination processes. *Development*, *138*(9), 1827–1838. <https://doi.org/10.1242/dev.053645>
- Roland, A. B., Ricobaraza, A., Carrel, D., Jordan, B. M., Rico, F., Simon, A., Humbert-Claude, M., Ferrier, J., McFadden, M. H., Scheuring, S., & Lenkei, Z. (2014). Cannabinoid-induced actomyosin contractility shapes neuronal morphology and growth. *ELife*, *3*, e03159. <https://doi.org/10.7554/eLife.03159>
- Roycroft, A., & Mayor, R. (2016). Molecular basis of contact inhibition of locomotion. *Cellular and Molecular Life Sciences*, *73*(6), 1119–1130. <https://doi.org/10.1007/s00018-015-2090-0>
- Saadat, S., Nouredini, M., Mahjoubin-Tehran, M., Nazemi, S., Shojaie, L., Aschner, M., Maleki, B., Abbasi-kolli, M., Rajabi Moghadam, H., Alani, B., & Mirzaei, H. (2021). Pivotal Role of TGF- β /Smad Signaling in Cardiac Fibrosis: Non-coding RNAs as Effectual Players. *Frontiers in Cardiovascular Medicine*, *7*, 588347. <https://doi.org/10.3389/fcvm.2020.588347>
- Sadaghiani, B., & Thiébaud, C. H. (1987). Neural crest development in the *Xenopus laevis* embryo, studied by interspecific transplantation and scanning electron microscopy. *Developmental Biology*, *124*(1), 91–110. [https://doi.org/10.1016/0012-1606\(87\)90463-5](https://doi.org/10.1016/0012-1606(87)90463-5)
- Sard, H., Kumaran, G., Morency, C., Roth, B. L., Toth, B. A., He, P., & Shuster, L. (2005). SAR of psilocybin analogs: Discovery of a selective 5-HT_{2C} agonist. *Bioorganic & Medicinal Chemistry Letters*, *15*(20), 4555–4559. <https://doi.org/10.1016/j.bmcl.2005.06.104>
- Schilling, T. F., & Kimmel, C. B. (1994). Segment and cell type lineage restrictions during pharyngeal arch development in the zebrafish embryo. *Development*, *120*(3), 483–494. <https://doi.org/10.1242/dev.120.3.483>

- Sechrist, J., Serbedzija, G. N., Scherson, T., Fraser, S. E., & Bronner-Fraser, M. (1993). Segmental migration of the hindbrain neural crest does not arise from its segmental generation. *Development*, *118*(3), 691–703. <https://doi.org/10.1242/dev.118.3.691>
- Shellard, A., Szabó, A., Trepát, X., & Mayor, R. (2018). Supracellular contraction at the rear of neural crest cell groups drives collective chemotaxis. *Science*, *362*(6412), 339–343. <https://doi.org/10.1126/science.aau3301>
- Shiau, C. E., Lwigale, P. Y., Das, R. M., Wilson, S. A., & Bronner-Fraser, M. (2008). Robo2-Slit1 dependent cell-cell interactions mediate assembly of the trigeminal ganglion. *Nature Neuroscience*, *11*(3), 269–276. <https://doi.org/10.1038/nn2051>
- Shoval, I., Ludwig, A., & Kalcheim, C. (2007). Antagonistic roles of full-length N-cadherin and its soluble BMP cleavage product in neural crest delamination. *Development*, *134*(3), 491–501. <https://doi.org/10.1242/dev.02742>
- Siismets, E. M., & Hatch, N. E. (2020). Cranial Neural Crest Cells and Their Role in the Pathogenesis of Craniofacial Anomalies and Coronal Craniosynostosis. *Journal of Developmental Biology*, *8*(3), 18. <https://doi.org/10.3390/jdb8030018>
- Silver, R. J. (2019). The Endocannabinoid System of Animals. *Animals*, *9*(9), 686. <https://doi.org/10.3390/ani9090686>
- Simon, E., Thézé, N., Fédou, S., Thiébaud, P., & Faucheux, C. (2017). Vestigial-like 3 is a novel Ets1 interacting partner and regulates trigeminal nerve formation and cranial neural crest migration. *Biology Open*, bio.026153. <https://doi.org/10.1242/bio.026153>
- Straight, A. F., Cheung, A., Limouze, J., Chen, I., Westwood, N. J., Sellers, J. R., & Mitchison, T. J. (2003). Dissecting Temporal and Spatial Control of Cytokinesis with a Myosin II Inhibitor. *Science*, *299*(5613), 1743–1747. <https://doi.org/10.1126/science.1081412>

- Taylor, A. H., Ang, C., Bell, S. C., & Konje, J. C. (2007). The role of the endocannabinoid system in gametogenesis, implantation and early pregnancy. *Human Reproduction Update*, 13(5), 501–513. <https://doi.org/10.1093/humupd/dmm018>
- The Endogenous Cannabinoid System: A Budding Source of Targets for Treating Inflammatory and Neuropathic Pain—PMC*. (n.d.). Retrieved December 12, 2022, from <https://www.ncbi.nlm.nih.gov/pmc/articles/PMC5719110/>
- Théveneau, E., Duband, J.-L., & Altabef, M. (2007). Ets-1 Confers Cranial Features on Neural Crest Delamination. *PLoS ONE*, 2(11), e1142. <https://doi.org/10.1371/journal.pone.0001142>
- Theveneau, E., & Mayor, R. (2012). Neural crest delamination and migration: From epithelium-to-mesenchyme transition to collective cell migration. *Developmental Biology*, 366(1), 34–54. <https://doi.org/10.1016/j.ydbio.2011.12.041>
- Tosney, K. W. (1982). The segregation and early migration of cranial neural crest cells in the avian embryo. *Developmental Biology*, 89(1), 13–24. [https://doi.org/10.1016/0012-1606\(82\)90289-5](https://doi.org/10.1016/0012-1606(82)90289-5)
- Trainor, P. A. (2005). Specification and Patterning of Neural Crest Cells During Craniofacial Development. *Brain, Behavior and Evolution*, 66(4), 266–280. <https://doi.org/10.1159/000088130>
- Trainor, P. A., & Tam, P. P. (1995). Cranial paraxial mesoderm and neural crest cells of the mouse embryo: Co-distribution in the craniofacial mesenchyme but distinct segregation in branchial arches. *Development*, 121(8), 2569–2582. <https://doi.org/10.1242/dev.121.8.2569>
- Waldo, K. L., Kumiski, D., & Kirby, M. L. (1996). Cardiac neural crest is essential for the persistence rather than the formation of an arch artery. *Developmental Dynamics*, 205(3), 281–292. [https://doi.org/10.1002/\(SICI\)1097-0177\(199603\)205:3<281::AID-AJA8>3.0.CO;2-E](https://doi.org/10.1002/(SICI)1097-0177(199603)205:3<281::AID-AJA8>3.0.CO;2-E)

- Waldo, K. L., Willner, W., & Kirby, M. L. (1990). Origin of the proximal coronary artery stems and a review of ventricular vascularization in the chick embryo. *American Journal of Anatomy*, 188(2), 109–120. <https://doi.org/10.1002/aja.1001880202>
- Waldo, K., Miyagawa-Tomita, S., Kumiski, D., & Kirby, M. L. (1998). Cardiac Neural Crest Cells Provide New Insight into Septation of the Cardiac Outflow Tract: Aortic Sac to Ventricular Septal Closure. *Developmental Biology*, 196(2), 129–144. <https://doi.org/10.1006/dbio.1998.8860>
- Wang, J., Xiao, Y., Hsu, C.-W., Martinez-Traverso, I. M., Zhang, M., Bai, Y., Ishii, M., Maxson, R. E., Olson, E. N., Dickinson, M. E., Wythe, J. D., & Martin, J. F. (2016). Yap and Taz play a crucial role in neural crest-derived craniofacial development. *Development (Cambridge, England)*, 143(3), 504–515. <https://doi.org/10.1242/dev.126920>
- Watson, S., Chambers, D., Hobbs, C., Doherty, P., & Graham, A. (2008). The endocannabinoid receptor, CB1, is required for normal axonal growth and fasciculation. *Molecular and Cellular Neuroscience*, 38(1), 89–97. <https://doi.org/10.1016/j.mcn.2008.02.001>
- Wu, C., & Taneyhill, L. A. (2019). Cadherin-7 mediates proper neural crest cell–placodal neuron interactions during trigeminal ganglion assembly. *Genesis*, 57(1), e23264. <https://doi.org/10.1002/dvg.23264>
- Xie, H., Sun, X., Piao, Y., Jegga, A. G., Handwerger, S., Ko, M. S. H., & Dey, S. K. (2012). Silencing or Amplification of Endocannabinoid Signaling in Blastocysts via CB1 Compromises Trophoblast Cell Migration. *Journal of Biological Chemistry*, 287(38), 32288–32297. <https://doi.org/10.1074/jbc.M112.381145>

Zheng, X., Suzuki, T., Takahashi, C., Nishida, E., & Kusakabe, M. (2015). *Cnrip1* is a regulator of eye and neural development in *Xenopus laevis*. *Genes to Cells*, 20(4), 324–339.

<https://doi.org/10.1111/gtc.12225>